To date, interferon (IFN)-γ receptor 1 (*IFNGR1*) [13–15], IFN-γ receptor 2 (*IFNGR2*) [16], interleukin (IL)-12 p40 subunit (*IL12B*) [17], IL-12 receptor β subunit (*IL12RB1*) [18–20], signal transducer and activator of transcription-1 (*STAT1*) [21], and nuclear factor-κB-essential modulator (*NEMO*) [22] mutations were identified as the causes of this primary immunodeficiency. On the other hand, no genetic etiology has yet been reported to be identified for about half of all patients with MSMD [3]. In addition, there have been no precise reports on the clinical characteristics and genetic backgrounds of MSMD in Asian countries, including Japan, which has a high prevalence of tuberculosis.

In this study, we analyzed patients who had a recurrent or disseminated infection with intracellular pathogens to clarify the clinical manifestations and host genetic backgrounds of MSMD in Japan.

Materials and Methods

Subjects

We studied 46 patients (30 males and 16 females) diagnosed as having MSMD because of recurrent infections, or blood-borne infections such as osteomyelitis/arthritis, and multiple infections at different anatomic sites by intracellular bacteria including BCG, NTM, *Salmonella* species, *Listeria monocytogenes*, or *M. tuberculosis* in 34 hospitals in Japan from 1999 to 2009. There was no consanguinity in these families. The clinical information on each patient was collected using a standardized case report form. Informed consent was obtained from the parents of the subjects before the study. This study was approved by the Ethics Committee of Kyushu University.

Flow Cytometric Analysis

Two-color flow cytometric analysis was performed to investigate IFN-γ receptor 1 (IFN-γR1) expression levels on the patients' monocytes by using an EPICS XL instrument (Beckman Coulter, Miami, FL, USA). Peripheral blood mononuclear cells (PBMCs) were stained with mouse anti-IFN-γR1 monoclonal antibody (MAb) (Genzyme, Cambridge, MA, USA), followed by rat phycoerythrin anti-mouse immunoglobulin antibody (BD Bioscience Pharmingen, San Diego, CA, USA). Cells were washed twice and stained with a phycoerythrin 5.1 (PC5)-anti-CD14 MAb (Beckman Coulter). IFN-γR1 expression was analyzed on monocytes determined by their side scatter and CD14 positivity.

Genomic DNA and cDNA Sequence Analysis

The *IFNGR1*, *IFNGR2*, *IL12B*, *IL12RB1*, *STAT1*, and *NEMO* genes were analyzed for coding exons and flanking intronic sequences. These genes were amplified by polymerase chain reaction (PCR) after whole genome amplification with a GenomiPhi V2 DNA Amplification Kit (GE Healthcare, Little Chalfont, UK). The PCR products were treated with an Exo-SAP-IT kit (GE Healthcare, Amersham, UK) and then were analyzed by direct sequencing with an ABI 3130 DNA sequencer (Perkin-Elmer, Foster City, CA, USA). Detected mutations were confirmed by sequencing the PCR product using cDNA as a template.

Statistical Analysis

Comparisons of the proportions were analyzed by the χ^2 test. The Mann–Whitney *U* test was used to compare differences between quantitative variables. A *P* value less than 0.05 was considered to be statistically significant.

Results

The median age of the patients was 8 years (range, 6 months–41 years), and the median age at the onset of infection was 1 year and 4 months (range, 4 months–6 years). The male to female ratio was 1.9:1. Only one patient had not received a BCG vaccination. There were 59 episodes of disseminated mycobacterial infections in the 46 patients. Nine (19%) of 46 patients had two or more episodes of these infections. Two of the patients had three episodes, and one had four episodes of these infections. In all episodes, BCG was the most common pathogen (82.6%, Table I). The *Mycobacterium avium* complex (MAC) was isolated during eight episodes of these infections. *M. tuberculosis* was also confirmed in two episodes of infection. No severe *Salmonella* species, *L. monocytogenes*, or viral infections were observed.

The common clinical manifestations were osteomyelitis/arthritis, lymphadenitis, and subcutaneous abscess/dermatitis (Table I and Fig. 1a). Only one patient was diagnosed as having arthritis, and the lesion spread to the adjacent bone. Two patients showed hepatosplenomegaly during the BCG infection, and two patients with the MAC infection developed pulmonary abscess. Among the BCG infections, the median intervals of time between BCG vaccination and the development of primary BCG infection were 3 (1–10 months), 4 (2–36 months), and 11 months (5–46 months) for the subcutaneous abscess/dermatitis, lymphadenitis, and osteomyelitis/arthritis, respectively (Fig. 1b).

We performed the genetic analysis on these patients for the *IFNGR1*, *IFNGR2*, *IL12B*, *IL12RB1*, *STAT1*, and *NEMO* genes. Six patients (five families) and one patient had mutations in the *IFNGR1* and *NEMO* genes, respectively (Table II). Five of the seven patients who had a mutation in the *IFNGR1* gene were the patients that we

Table I The clinical manifestations of the patients with MSMD

	Patients with genetic mutation, *n* (%)	Patients without a genetic mutation, *n* (%)	Total *n* (%)
Causative pathogen[a]			
BCG	3 (42.9)	35 (89.7)	38 (82.6)
M. avium complex	1 (14.3)	3 (10.2)	4 (8.7)
BCG+*M. avium* complex	2 (28.5)	0 (0)	2 (4.3)
M. avium complex+*M. tuberculosis*	1 (14.3)	1 (2.6)	2 (4.3)
Sites of infection[b]			
Osteomyelitis/arthritis	7 (43.8)	24 (55.8)	31 (52.5)
Lymphadenitis	8 (50.0)	8 (18.6)	16 (27.1)
Dermatitis/subcutaneous	3 (18.8)	11 (25.6)	14 (23.7)
Pulmonary abscess	0 (0)	2 (4.7)	2 (3.4)

The total number exceeds 59 because some patients had multiple lesions at the same time

[a] $n=7$ for patients with a genetic mutation and $n=39$ for patients without a genetic mutation

[b] $n=16$ for patients with a genetic mutation and $n=43$ for patients without a genetic mutation

reported previously [14, 15], and the other two patients were newly identified. All of the IFN-γR1-deficient patients were heterozygotes, and the mutation was in the transmembrane domain in one patient (774del4: patient 5) and in the intracellular domain in five patients (811del4: patient 1, 818del4: patients 2–4, and 832 G>T, E278X: patient 6), which led to the expression of a truncated protein with a dominant negative effect on the IFN-γR1 signaling (Table II and Fig. 2a). The IFN-γR1 expression levels were significantly increased in all six patients with IFN-γR1 deficiency (Fig. 2b). Patient 7 had a missense mutation in *NEMO* (943 G>C, E315Q). The CD14-positive cells from this patient produced a lower level of TNF in response to LPS stimulation (data not shown), which was consistent with the defect in NF-κB signaling.

The proportions of the patients with recurrent mycobacterial infection or multiple osteomyelitis/arthritis were

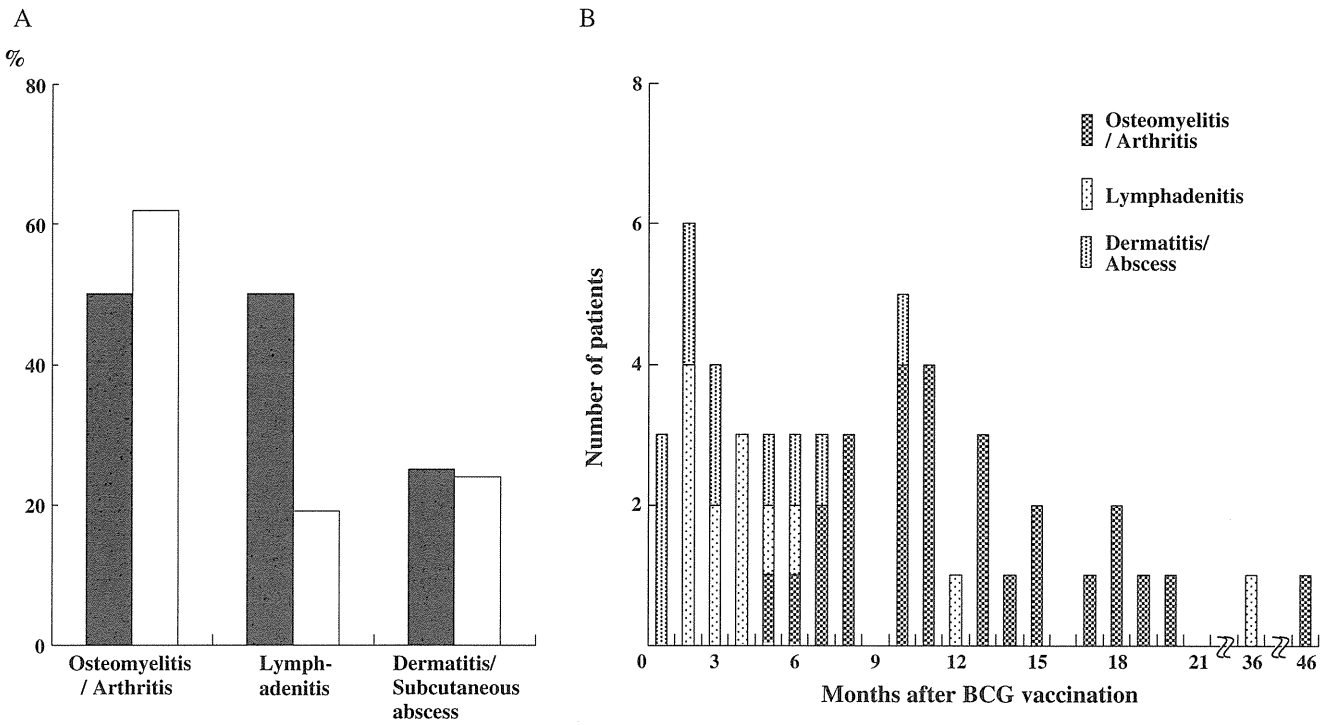

Fig. 1 The clinical features of the patients with BCG infection. The distribution of the sites of infections (**a**) and the intervals between BCG vaccination and the first onset of BCG infection (**b**) are shown. The *black bar* and the *white bar* represent the proportion of the patients with and without genetic mutations, respectively

Table II Characteristics of the patients with a genetic mutation

Patient no.	Sex	Age	Age of onset	Episodes of infections prior to detection of the genetic mutation	Genetic mutation
1[a] [14]	F	1 year 7 months	10 months	BCG lymphadenitis and dermatitis Multiple BCG osteomyelitis	*IFNGR1* 811del4
2[a] [14]	M	1 year 9 months	8 months	BCG lymphadenitis, hepatomegaly Multiple BCG osteomyelitis	*IFNGR1* 818del4
3[a] [14]	M	2 years	2 years	Multiple BCG osteomyelitis	*IFNGR1* 818del4
4[a] [14]	M	41 years	3 years	*M. tuberculosis* lymphadenitis (twice) Multiple MAC octeomyelitis	*IFNGR1* 818del4
5[a] [15]	F	12 years	6 months	BCG lymphadenitis Multiple MAN osteomyelitis	*IFNGR1* 774del4
6	M	19 years	4 months	BCG lymphadenitis and dermatitis Multiple BCG osteomyelitis MAC subcutaneous abscess Multiple MAC osteomyelitis	*IFNGR1* E278X
7	M	10 years	10 months	*M. tuberculosis* lymphadenitis Multiple MAC lymphadenitis Sepsis, bacterial pneumonia (four times)	*NEMO* E315Q

Patient 4 is the father of patient 2

MAC Mycobacterium avium complex

[a] These patients were reported previously

significantly higher in those with the genetic mutations (Table III). There were no significant differences in the age at the onset of mycobacterial infection, or in the interval of time between BCG vaccination and the first onset of BCG infection between the patients with and without genetic mutations. One patient diagnosed with BCG dermatitis died of persistent diarrhea of unknown etiology, while the others are still alive.

Discussion

In the present study, we investigated the clinical characteristics and the genetic backgrounds of the patients diagnosed as having MSMD in Japan. We observed that the patients with the genetic mutation were susceptible to developing recurrent mycobacterial infections and multiple osteomyelitis/arthritis, and IFN-γR1 deficiency was the most

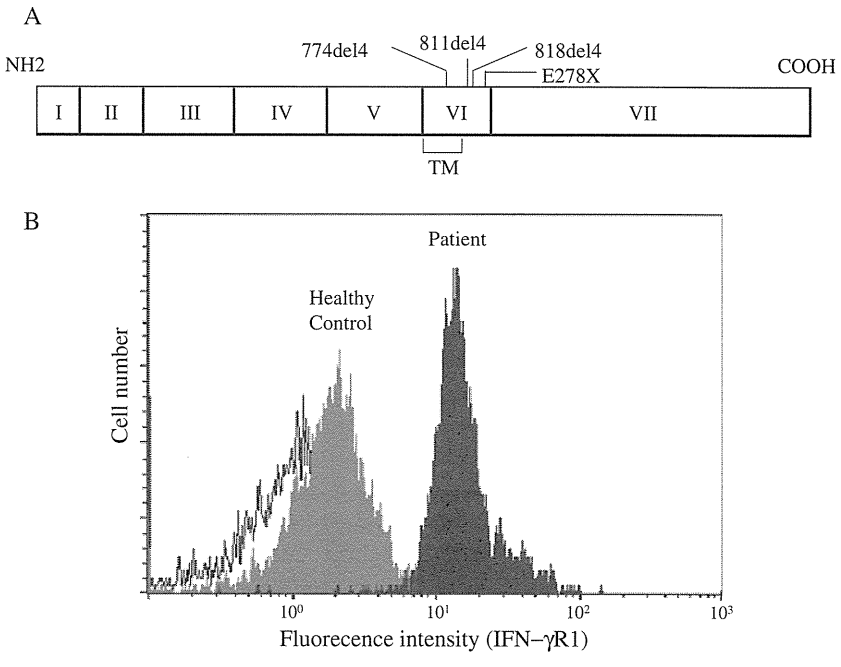

Fig. 2 *IFNGR1* gene mutations and the analysis of IFN-γR1 expression on monocytes. The sites of *IFNGR1* gene mutations in the six IFN-γR1-deficient patients (**a**) and the increased IFN-γR1 expression level on monocytes in patient 2 are shown (**b**)

Table III Comparison of the patients with and without a genetic mutation

	Patients with a genetic mutation (n=7)	Patients without a genetic mutation (n=39)
Age of onset (months)	10 (4–36)	14 (4–75)
Male to female ratio	2.5:1	1.8:1
Familial history (n)	2	0
Median interval between BCG vaccination and the first onset of BCG infection (months)	9.5 (7–15, n=4)	10 (1–46, n=35)
Recurrent cases (%)	85.7*	7.7
Patients with multiple osteomyelitis/arthritis (%)	100* (n=6)	4.2 (n=24)

*p<0.0001

frequent genetic defect identified in these patients. The prevalence of MSMD is estimated to be at least 0.59 cases per million births, and the disease does not seem to be confined to any ethnic group or geographic region, according to a national retrospective study of idiopathic disseminated BCG infection in France [23, 24]. This is the first epidemiological study associated with MSMD in Japan which showed the difference in the clinical manifestation and the genetic background between Japan and Western countries.

The *IFNGR1* mutations identified in this study were in exon IV, within the transmembrane domain, or the intracellular domain of the *IFNGR1* gene (Fig. 2a), which led to a truncated protein lacking signaling motifs [25]. The truncated protein also lacks the recycling motif, which leads to the overexpression of the mutant protein (Fig. 2b) [25]. These mutations are located in important hot spots in the patients diagnosed with dominant partial IFN-γR1 deficiency [13], and the flow cytometric analysis of IFN-γR1 expression levels may be a useful method for the screening for this disease [15]. The *NEMO* mutation found in patient 7 was in exon VIII within the leucine zipper domain of the *NEMO* gene. A previous study reported that a mutation in this region disrupted a common salt bridge in the leucine zipper domain and impaired T-cell-dependent IL-12 production [22].

The patients with the genetic mutations were susceptible to recurrent mycobacterial infections and multiple osteomyelitis/arthritis as described previously [3], but no fatal mycobacterial infection was observed in this study. Unlike complete IFN-γR1 and IFN-γR2 deficiencies, which often cause fatal mycobacterial infections [13, 16], the patients with dominant partial IFN-γR1 and NEMO deficiencies have been reported to have a relatively mild disease and a better prognosis [13, 22]. These factors might have contributed to the good outcome of the patients in this study. In addition, the low virulence of BCG might contribute to the characteristics of BCG infection in Japan, because the BCG Tokyo 172 strain that is used in Japan for vaccination is the least virulent BCG substrain.

The *IL12RB1* mutation has been reported to be the most common cause of MSMD [4]. However, none of the patients in this study was diagnosed as having an IL-12 receptor β1 deficiency. In Japan, this disease was reported in only one patient with disseminated lymphadenitis caused by *M. avium* complex [18]. It has been suggested that most complete IL-12 receptor β1-deficient individuals may be asymptomatic, and only those that also have a second mutation in another gene may be more prone to infections [26, 27]. These symptomatic IL-12 receptor β1-deficient patients are mainly found in families with consanguineous parents [19, 27]. Consanguineous marriages are uncommon in Japan, and there were no consanguineous families in this study. This might be the reason why no IL-12 receptor β1-deficient patients were observed. Alternatively, it is possible that the causative gene mutations associated with MSMD are different among races, because the number of patients with IL-12 receptor β1 deficiency was also lower than those with IFN-γR1 deficiency in Taiwan [28].

Although another patient had multiple osteomyelitis, and three patients had recurrent disseminated mycobacterial infections in these studies, they did not have mutations in any of the six genes. It was previously reported that no genetic etiology has yet been identified in about half of patients with disseminated and recurrent mycobacterial infections [3, 4]. This suggests the presence of as yet undetermined genetic factors in the development of this disease.

In the present study, the number of patients with genetic mutations might be too small to conclusively indicate the differences in the clinical manifestations and the host genetic backgrounds of MSMD between Japan and Western countries. However, in terms of the genetic etiology and the prognosis, it remains possible that the features of the patients diagnosed as having MSMD in the present study are different from those in previous reports [3]. Further investigations of a large number of patients are therefore warranted to more precisely evaluate the clinical manifestations and the host genetic background of MSMD in Japan.

Conclusions

We found that the patients diagnosed as having MSMD in Japan seem to have different genetic features, as well as

different clinical manifestations, compared with those in Western countries. A few patients with recurrent mycobacterial infections without mutations in the six known genes might suggest a contribution of other genetic, as well as environmental, factors in the susceptibility to recurrent infections.

Acknowledgments We thank the physicians for providing detailed information and allowing us to analyze blood samples of the MSMD patients, and we appreciate the assistance of Dr. Brain Quinn for editing the English usage. This study was supported in part by the Ministry of Education, Culture, Sports, Science and Technology of Japan, and by a grant for Research on Intractable Diseases from the Ministry of Health, Labor and Welfare of Japan.

References

1. Ottenhoff TH, Verreck FA, Hoeve MA, van de Vosse E. Control of human host immunity to mycobacteria. Tuberculosis. 2005;85:74–5.
2. Hamosh A, Scott AF, Amberger JS, Bocchini CA, McKusick VA. Online Mendelian Inheritance in Man (OMIM), a knowledgebase of human genes and genetic disorders. Nucl Acids Res. 2005;33: D514–7.
3. Al-Muhsen S, Casanova JL. The genetic heterogeneity of Mendelian susceptibility to mycobacterial diseases. J Allergy Clin Immunol. 2008;122:1043–51.
4. Filipe-Santos O, Bustamante J, Chapgier A, Vogt G, de Beaucoudrey L, Feinberg J, et al. Inborn errors of IL-12/23- and IFN-γ-mediated immunity: molecular, cellular, and clinical features. Semin Immunol. 2006;18:347–61.
5. Alcais A, Fieschi C, Abel L, Casanoca JL. Tuberculosis in children and adults: two distinct genetic diseases. J Exp Med. 2005;202:1617–21.
6. Casanova JL, Abel L. Genetic dissection of immunity to mycobacteria: the human model. Annu Rev Immunol. 2002;20:581–620.
7. Picard C, Fieschi C, Altare F, Al-Jumaah S, Al-Hajjar S, Feinberg J, et al. Inherited interleukin-12 deficiency: IL12B genotype and clinical phenotype of 13 patients from six kindreds. Am J Hum Genet. 2002;70:336–48.
8. Roesler J, Kofink B, Wendisch J, Heyden S, Paul D, Friedrich W, et al. *Listeria monocytogenes* and recurrent mycobacterial infections in a child with complete interferon-gamma-receptor (IFNgammaR1) deficiency: mutational analysis and evaluation of therapeutic options. Exp Hematol. 1999;27:1368–74.
9. Moraes-Vasconcelos D, Grumach AS, Yamaguti A, Andrade ME, Fieschi C, de Beaucoudrey L, et al. *Paracoccidioides brasiliensis* disseminated disease in a patient with inherited deficiency in the beta 1 subunit of the interleukin (IL)-12/IL-23 receptor. Clin Infect Dis. 2005;41:e31–7.
10. Zerbe CS, Holland SM. Disseminated histoplasmosis in persons with interferon gamma receptor 1 deficiency. Clin Infect Dis. 2005;41:e38–41.
11. Sanal O, Turkkani G, Gumruk F, Yel L, Secmeer G, Tezcan I, et al. A case of interleukin-12 receptor beta-1 deficiency with recurrent leishmaniasis. Pediatr Infect Dis. 2007;26:366–8.
12. Camcioglu Y, Picard C, Lacoste V, Dupuis S, Akçakaya N, Cokura H, et al. HHV-8-associated Kaposi sarcoma in a child with IFNgammaR1 deficiency. J Pediatr. 2004;144:519–23.
13. Doman SE, Picard C, Lammas D, Heyne K, van Dissel JT, Baretto R, et al. Clinical features of dominant and recessive interferon γ receptor 1 deficiencies. Lancet. 2004;364:2113–21.
14. Sasaki Y, Nomura A, Kusuhara K, Takada H, Ahmed S, Obinata K, et al. Genetic basis of patients with bacille Calmette-Guerin osteomyelitis in Japan: identification of dominant partial interferon-gamma receptor 1 deficiency as a predominant type. J Infect Dis. 2002;185:706–9.
15. Okada S, Ishikawa N, Shirao K, Kawaguchi H, Tsumura M, Ohno Y, et al. The novel IFNGR1 mutation 774del4 produces a truncated form of interferon-γ receptor 1 and has a dominant-negative effect on interferon-γ signal transduction. J Med Genet. 2007;44:485–91.
16. Dorman SE, Holland SM. Mutation in the signal-transducing chain of the interferon-γ receptor and susceptibility to mycobacterial infection. J Clin Invest. 1998;101:2364–9.
17. Altare F, Lammas D, Revy P, Jouanguy E, Döffinger R, Lamhamedi S, et al. Inherited interleukin-12 deficiency in a child with bacille Calmette-Guerin and *Salmonella enteritidis*-disseminated infection. J Clin Invest. 1998;102:2035–40.
18. Sakai T, Matsuoka M, Aoki M, Nosaka K, Mitsuya H. Missense mutation of the interluekin-12 receptor β1 chain-encoding gene is associated with impaired immunity against *Mycobacterium avium complex* infection. Blood. 2001;97:2688–94.
19. Raspall M, Da Silva Duarte AJ, Tuerlinckx D, Virelizier JL, Fischer A, Enright A, et al. Low penetrance, broad resistance, and favorable outcome of interleukin 12 receptor β1 deficiency: medical and immunological implications. J Exp Med. 2003;197:527–35.
20. van de Vosse E, Ottenhoff THM. Human host genetic factors in mycobacterial and *Salmonella* infection: lessons from single gene disorders in IL12/IL-12-dependent signaling that affect innate and adaptive immunity. Microb Infect. 2006;8:1167–73.
21. Dupuis S, Dargemont C, Fieschi C, Thomassin N, Rosenzweig S, Harris J, et al. Impairment of mycobacterial but not viral immunity by a germline human STAT1 mutation. Science. 2001;293:300–3.
22. Filipe-Santos O, Bustamante J, Haverkamp MH, Vinolo E, Ku CL, Puel A, et al. X-linked susceptibility to mycobacteria is caused by mutations in NEMO impairing CD40-dependent IL-12 production. J Exp Med. 2006;203:1745–59.
23. Casanova JL, Jouanguy E. Immunological conditions of children with BCG disseminated infection. Lancet. 1995;346:581.
24. Casanova JL, Blanche S, Emile JF, Jouanguy E, Lamhamedi S, Altare F, et al. Idiopathic disseminated bacille Calmette-Guerin infection: a French national retrospective study. Pediatrics. 1996;98:774–8.
25. Jouanguy E, Lamhamedi-Cherradi S, Lammas D, Dorman SE, Fondanèche MC, Dupuis S, et al. A human IFN-γR1 small deletion hotspot associated with dominant susceptibility to mycobacterial infection. Nat Genet. 1999;21:370–8.
26. van de Vosse E, Ottenhoff THM. Human host genetic factors in mycobacterial and *Salmonella* infection: lessons from single gene disorders in IL-12/IL-23-dependent signaling that affect innate and adaptive immunity. Microbes Infect. 2006;8:1167–73.
27. Ehlayel M, de Beaucoudrey L, Fike F, Nahas SA, Feinberg J, Casanova JL, et al. Simultaneous presentation of 2 rare hereditary immunodeficiencies: IL-12 receptor β1 deficiency and ataxia-telangiectasia. J Allergy Clin Immunol. 2008;122:1217–9.
28. Lee WI, Huang JL, Lin TY, Hsueh C, Wong AM, Hsieh MY, et al. Chinese patients with defective IL-12/23-interferon γ receptor 1 mutation presenting as cutaneous granuloma and IL12 receptor β1 mutation as pneumatocele. J Clin Immunol. 2009;29:238–45.

Hoxb4 transduction down-regulates Geminin protein, providing hematopoietic stem and progenitor cells with proliferation potential

Yoshinori Ohno[a,1], Shin'ichiro Yasunaga[a,1], Motoaki Ohtsubo[a], Sayaka Mori[a], Miyuki Tsumura[a,b], Satoshi Okada[a,b], Tomohiko Ohta[c], Kiyoshi Ohtani[d], Masao Kobayashi[b], and Yoshihiro Takihara[a,2]

[a]Department of Stem Cell Biology, Research Institute for Radiation Biology and Medicine, Hiroshima University, Hiroshima 734-8553, Japan; [b]Department of Pediatrics, Hiroshima University Graduate School of Biomedical Sciences, Hiroshima 734-8551, Japan; [c]Division of Breast and Endocrine Surgery, St. Marianna University School of Medicine, Kawasaki 216-8511, Japan; and [d]Department of Bioscience, School of Science and Technology, Kwansei Gakuin University, Sanda 669-1337, Japan

Edited* by Tak Wah Mak, The Campbell Family Institute for Breast Cancer Research, Ontario Cancer Institute at Princess Margaret Hospital, University Health Network, Toronto, Canada, and approved October 26, 2010 (received for review July 28, 2010)

Retrovirus-mediated transduction of Hoxb4 enhances hematopoietic stem cell (HSC) activity and enforced expression of Hoxb4 induces in vitro development of HSCs from differentiating mouse embryonic stem cells, but the underlying molecular mechanism remains unclear. We previously showed that the HSC activity was abrogated by accumulated Geminin, an inhibitor for the DNA replication licensing factor Cdt1 in mice deficient in *Rae28* (also known as *Phc1*), which encodes a member of Polycomb-group complex 1. In this study we found that Hoxb4 transduction reduced accumulated Geminin in *Rae28*-deficient mice, despite increasing the mRNA, and restored the impaired HSC activity. Supertransduction of Geminin suppressed the HSC activity induced by Hoxb4 transduction, whereas knockdown of Geminin promoted the clonogenic and replating activities, indicating the importance of Geminin regulation in the molecular mechanism underlying Hoxb4 transduction-mediated enhancement of the HSC activity. This facilitated our investigation of how transduced Hoxb4 reduced Geminin. We showed in vitro and in vivo that Hoxb4 and the Roc1 (also known as Rbx1)-Ddb1-Cul4a ubiquitin ligase core component formed a complex designated as RDCOXB4, which acted as an E3 ubiquitin ligase for Geminin and down-regulated Geminin through the ubiquitin-proteasome system. Down-regulated Geminin and the resultant E2F activation may provide cells with proliferation potential by increasing a DNA prereplicative complex loaded onto chromatin. Here we suggest that transduced Hoxb4 down-regulates Geminin protein probably by constituting the E3 ubiquitin ligase for Geminin to provide hematopoietic stem and progenitor cells with proliferation potential.

Retrovirus-mediated transduction of Hoxb4 has been shown to enhance activities of hematopoietic stem cells (HSCs), including self-renewal capacity in vivo and ex vivo in mice and humans (1–3). Moreover, enforced expression of Hoxb4 induces in vitro development of HSCs from differentiating mouse embryonic stem cells on OP9 stroma, suggesting that Hoxb4 also promotes developmental maturation of HSCs (4). It has therefore been anticipated that Hoxb4 can aid the development of a technological procedure for preparing a sufficient number of HSCs ex vivo (5, 6) as well as elucidate the molecular mechanism supporting HSC activity. Hox genes are widely conserved and share a homeobox encoding the homeodomain. Because the homeobox was ascertained to provide a sequence-specific DNA-binding activity, Hox genes have long been believed to specify antero-posterior positional identity through their transcriptional regulatory activity (7). Hoxb4 with an N-to-A substitution at amino acid 212 within helix 3 of the homeodomain (Hoxb4N > A) lacks DNA-binding capacity and it cannot enhance HSC activity (8). This has supported the hypothesis that Hoxb4 enhances HSC activity through its transcriptional regulatory activity. It has been further reported that Hoxb4 transcriptionally activates *c-Myc* (also known as *Myc*) (9) and down-regulates genes involved in TNF-α and FGF signaling in bone marrow cells (BMCs) (10). The molecular mechanism underlying Hoxb4-mediated activation of HSCs, however, currently remains insufficiently understood.

Rae28 and Bmi1, members of Polycomb-group (PcG) complex 1, have been shown to be essential for sustaining HSC activity (11, 12). PcG complex 1 maintains the transcriptionally repressed state of Hox genes through ubiquitination of histone H2A at lysine 119 (13), and Hoxb4 is one of the downstream targets for PcG complex 1 during early development (14). It is, however, presumed that Hoxb4 does not act as a downstream mediator for PcG complex 1 in sustaining HSC activity because Hoxb4 expression was not affected in hematopoietic cells deficient in *Rae28* and *Bmi1* (11, 12). *Bmi1* was shown to maintain HSC activity through direct repression of the INK4a locus encoding the p16 cyclin-dependent kinase inhibitor and p19ARF (12, 15) as well as through direct interaction with E4F1 (16). p19ARF and E4F1 are known to regulate p53 through ubiquitination (17, 18). On the other hand, we recently demonstrated that PcG complex 1, consisting of Ring1B, Bmi1, Rae28, and Scmh1, functions as an E3 ubiquitin ligase for Geminin, an inhibitor of DNA replication licensing factor Cdt1 (19), and that abnormal accumulation of Geminin impairs HSC activity in *Rae28*-deficient ($Rae^{-/-}$) mice (20). In this study, we find that the impaired HSC activity in $Rae^{-/-}$ fetal liver cells (FLCs) was genetically complemented by Hoxb4 transduction and provide evidence suggesting that Hoxb4 acts as an E3 ubiquitin ligase for Geminin through the direct interaction with the Roc1-Ddb1-Cul4a ubiquitin ligase core component to regulate the protein's stability. Subsequently, down-regulated Geminin, in conjunction with its E2F activation, may facilitate DNA replication licensing to provide cells with proliferation potential (19). Geminin is further known to regulate chromatin remodeling (21) and transcription (22, 23). Here we indicate that Geminin regulation is crucial for Hoxb4 transduction-mediated enhancement of the hematopoietic stem and progenitor cell activity.

Results

Expression of Roc1, Ddb1, and Cul4a and Their Complex Formation with Hoxb4. Murine BMCs were sorted for purification of a $CD34^-$ $c\text{-}kit^+$ $Sca1^+$ lineage marker-negative (lin^-) subpopulation ($CD34^-KSL$)

Author contributions: Y.T. designed research; Y.O., S.Y., M.O., S.M., M.T., and S.O. performed research; T.O. and K.O. contributed new reagents/analytic tools; M.K. and Y.T. analyzed data; and Y.T. wrote the paper.

The authors declare no conflict of interest.

*This Direct Submission article had a prearranged editor.

[1]Y.O. and S.Y. contributed equally to this work.

[2]To whom correspondence should be addressed. E-mail: takihara@hiroshima-u.ac.jp.

This article contains supporting information online at www.pnas.org/lookup/suppl/doi:10.1073/pnas.1011054107/-/DCSupplemental.

[long-term repopulating (LTR)-HSCs], CD34$^+$KSL (multipotential progenitor cells), c-kit$^+$ Sca1$^-$ lin$^-$ cells (progenitors), and their progeny subpopulations. Expression of *Roc1*, *Ddb1*, and *Cul4a* was detected in each of the hematopoietic subpopulations by RT-PCR analysis (Fig. 1*A*). Although *Cul4a* expression was predominant in lymphoid cells, that in HSC and progenitor subpopulations is presumed to be functionally significant because the HSC activity was reportedly defective in the heterozygous *Cul4a*-deficient mice (24). Because the yeast two-hybrid analysis with Hoxb4 as bait and Cul4a as prey clearly suggested that Hoxb4 directly interacts with Cul4a (Fig. S1*A*) similarly to Hoxa9 (25), we examined whether Hoxb4 forms a complex (designated as RDCOXB4) with Roc1-Ddb1-Cul4a in a cell line derived from the human kidney cells, HEK-293 cells (HEK-293), transfected with Flag-tagged Hoxb4. Roc1, Cul4a, and Ddb1 were detected in the immunoprecipitates prepared with an anti-Flag antibody (Fig. 1*B*), indicating that exogeneous Hoxb4 formed the RDCOXB4 complex in HEK-293. The similar complex formation was observed in a Hoxb4-transduced myeloid cell line, 32D cells (32D) (Fig. S1*B*). The RDCOXB4 complex may directly interact with Geminin because the yeast two-hybrid and immunoprecipitation analyses showed that Hoxb4 interacted with Geminin through the homeodomain (Fig. S1 *G* and *H*) as the other Hox proteins did (22).

Hoxb4 Restores Impaired HSC Activity and Geminin Protein Level in Rae$^{-/-}$FLC. We then determined whether Hoxb4 compensated for impaired HSC activity in Rae$^{-/-}$ mice, which resulted from accumulated Geminin (20). Hoxb4 was transduced into wild-type FLC (Rae$^{+/+}$FLC) and Rae$^{-/-}$FLC by using a murine stem cell virus vector with the enhanced yellow fluorescence protein (EYFP) gene (MEP). Hoxb4 transduction increased cell population in the S phase, stopped apoptosis, and recovered the impaired clonogenic, long-term culture-initiating cell (LTC-IC) and LTR activities in Rae$^{-/-}$FLC, whereas Hoxb4N>A exerted little effect (Fig. S2 *A–D* and Fig. 2*A*). Because we previously showed that accumulated Geminin gave rise to HSC deficiency in Rae$^{-/-}$FLC, we next examined the effect of Hoxb4 transduction on Geminin. Although Geminin mRNA was increased by Hoxb4 transduction as similar to mRNAs for *Cdt1* and *Cyclin A2*, target genes for E2F (Fig. S2*E*), cell sorting analysis showed that Geminin protein was significantly reduced by Hoxb4 transduction in each phase of the cell cycle (Fig. 2*B*). Down-regulation of Geminin protein was also detected in Lin$^+$, KSL, and CD34$^-$KSL subpopulations of Hoxb4-transduced BMCs (Fig. S3). Down-regulation of Geminin protein was further confirmed by immunoblot analysis in Hoxb4-transduced BMCs and 32D where the mRNA and S-phase cells were increased (Fig. 2*C* and Fig. S1 *C–F*).

Effect of Geminin on Hoxb4-Mediated Hematopoietic Induction. To examine whether down-regulation of Geminin protein is involved in the molecular mechanism underlying the Hoxb4-mediated hematopoietic induction, we examined the effect of Geminin on Hoxb4-transduced BMCs. BMCs were first transduced with Hoxb4 by using the murine stem-cell virus vector with the resistance gene for puromycin (MPI) and then were supertransduced by using the MEP vector with either Geminin or destruction box-deleted Geminin (Geminin-DBD), which is resistant to ubiquitination by the anaphase-promoting complex/cyclosome (APC/C) (26). Geminin protein was reduced by Hoxb4 transduction throughout the cell cycle, and Geminin supertransduction reverted the reduced Geminin protein level to that in control cells (Fig. 3*A*). Transduction of Geminin-DBD further up-regulated Geminin

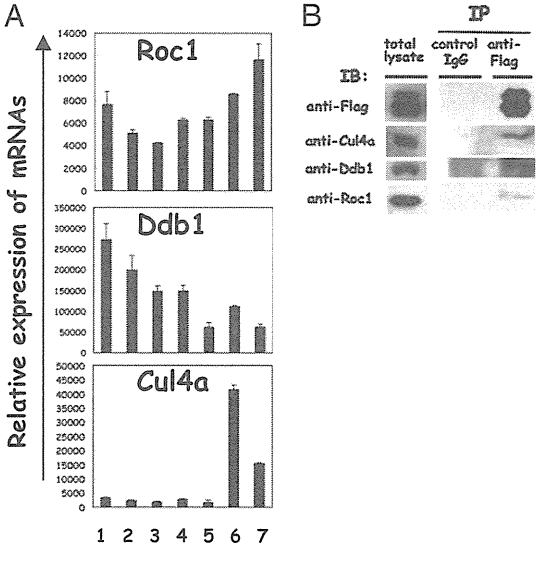

Fig. 1. Expression of Roc1, Ddb1, and Cul4a and the complex formation with Hoxb4. (*A*) mRNA expression examined by quantitative RT-PCR. The mRNA expression levels are shown as ratios to the level in GAPDH. 1, CD34$^-$KSL; 2, CD34$^+$KSL; 3, progenitors; 4, Ter119$^+$ cells (erythroid cells); 5, Gr1$^+$ cells (granulocytes); 6, CD3$^+$ cells (T cells); 7, B220$^+$ cells (B cells). (*B*) Immunoprecipitation analysis of the RDCOXB4 complex in HEK-293 transfected with Flag-Hoxb4. An anti-HA polyclonal antibody was used as a control antibody in the immunoprecipitation. IP, immunoprecipitation; IB, immunoblotting.

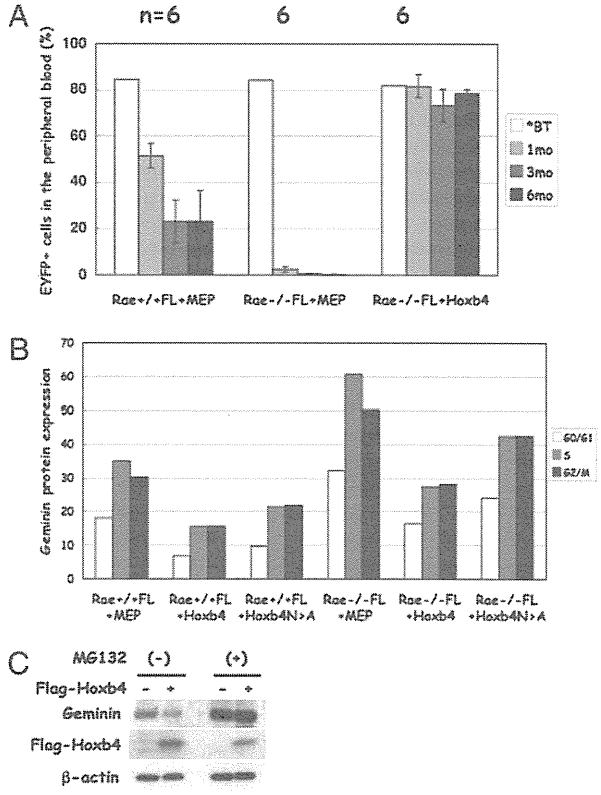

Fig. 2. Effect of Hoxb4 transduction on FLCs and BMCs. (*A*) LTR activity. Percentages of EYFP$^+$ cells in the peripheral blood cells of recipient mice were examined 1, 3, and 6 mo after transplantation. BT: before transplantation. Number of recipient mice is shown above the graph. (*B*) Geminin protein in FLCs, which were examined in each phase of the cell cycle by flow cytometry. (*C*) Geminin protein in BMCs, which were examined by immunoblot analysis. Hoxb4 transduction-mediated down-regulation of Geminin was suppressed by MG132 treatment.

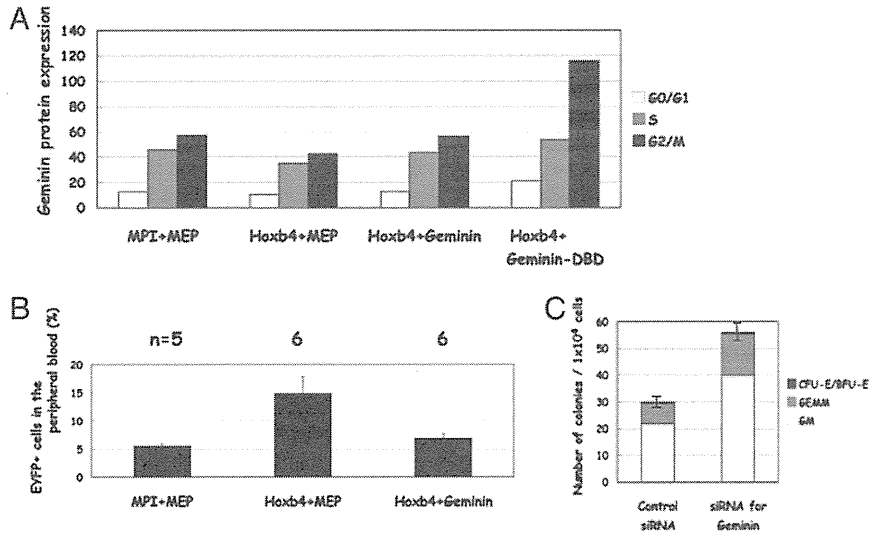

Fig. 3. Effect of Geminin transduction or knockdown in BMCs. (*A*) Effect of Geminin transduction on Geminin protein. BMCs were transduced with Hoxb4 and either Geminin or Geminin-DBD, and Geminin protein in each phase of the cell cycle was determined by flow cytometry. (*B*) Effect of Geminin transduction on LTR activity. (*C*) Effect of siRNA-induced Geminin knockdown on clonogenic activity.

protein (Fig. 3*A*). Geminin and Geminin-DBD transduction efficiently abrogated the clonogenic activity enhanced by Hoxb4 transduction (Fig. S4*A*). Geminin transduction also remarkably affected the replating, LTC-IC, and LTR activities enhanced by Hoxb4 transduction (Fig. 3*B* and Fig. S4 *B* and *C*). On the other hand, siRNA-mediated Geminin knockdown did not affect cell cycling (Fig. S5 *A* and *B*) but clearly promoted clonogenic and replating activities (Fig. 3*C* and Fig. S5 *C* and *D*). We further observed that the enhanced clonogenic activity was suppressed by restoration of Geminin (Fig. S5 *E* and *F*), confirming that the effect of the siRNA was mediated by specific down-regulation of Geminin. These findings indicated that Geminin down-regulation is crucial for Hoxb4-mediated induction of the HSC activity.

Effect of Hoxb4 on Geminin in HEK-293. We next examined the molecular mechanism of how Hoxb4 transduction down-regulated Geminin protein. Transient transfection of Hoxb4 reduced endogeneous Geminin protein in HEK-293 (Fig. 4*A*) despite increasing the mRNA (Fig. S6*A*), whereas the reduction was completely suppressed by treatment of MG132, an inhibitor of proteasome (Fig. 4*A*). Geminin down-regulation in Hoxb4-transduced BMCs and 32D was also suppressed by MG132 treatment (Fig. 2*C* and Fig. S1*F*). Pulse-chase–labeled Geminin with [^{35}S]methionine was shown to be destabilized in Hoxb4-transduced HEK-293 (Fig. S6*B*). Cul4a overexpression induced down-regulation of Geminin protein synergistically with Hoxb4 (Fig. S6*C*). siRNA-mediated knockdown of Cul4a eliminated the downregulating effect of Hoxb4 on Geminin protein (Fig. 4*B*), which facilitated our examination of the involvement of Cul4a in Hoxb4-mediated Geminin regulation. Mobility-shifted Geminin bands were detected in extracts from HEK-293 cotransfected with Geminin, hemagglutinin (HA)-tagged ubiquitin (HA-Ub), and Hoxb4 or Cul4a in the presence of MG132 (Fig. S7*A*). Mobility-shifted Geminin bands were confirmed to be ubiquitin-conjugated Geminin by means of immunoprecipitation analysis (Fig. S7*B*). Ubiquitination of Geminin-DBD through Hoxb4 was similar to that of Geminin (Fig. S7*A*), suggesting that the Hoxb4-mediated ubiquitination was independent of APC/C. The above-mentioned findings support a hypothesis that transduced Hoxb4 down-regulates Geminin protein through the ubiquitin-proteasome system (UPS) with the RDCOXB4 complex as the E3 ubiquitin ligase.

Reconstitution of E3 Ubiquitin Ligase Activity of RDCOXB4 for Geminin. To determine the E3 ubiquitin ligase activity of the RDCOXB4 complex for Geminin, we reconstituted the recombinant protein complex in *Spodoptera frugiperda* insect cells, named Sf9. Sf9 were coinfected with baculoviruses including His6-Roc1, Ddb1, Cul4a (27), and Flag-Hoxb4. Cell extracts were then prepared from Sf9-expressing (His6-Roc1)-Ddb1-Cul4a-(Flag-Hoxb4)[RDCOXB4], which was purified with metal affinity column chromatography. Gel filtration fractionation analysis showed that one of the peak fractions of Flag-Hoxb4 corresponded with the complex with a molecular weight similar to that of the recombinant complex consisting of stoichiometrically determined amounts of the components (260 kDa) (Fig. S8*A*). We also prepared and purified (GST-Roc1)-Ddb1-Cul4a-(Flag-Hoxb4) [RDCOXB4] with glutathione affinity column chromatography (Fig. 5*A*). The affinity-purified recombinant

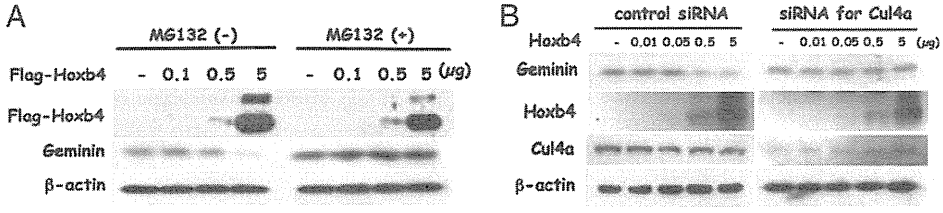

Fig. 4. Effect of Hoxb4 or Cul4a on Geminin protein in HEK-293. (*A*) Effect of Hoxb4 transfection on Geminin protein, which was examined by immunoblot analysis. The effect was suppressed by MG132 treatment. (*B*) Effect of Cul4a knockdown on Hoxb4-mediated down-regulation of Geminin protein.

RDCOXB4 was then subjected to an in vitro ubiquitination assay with purified bacterially produced recombinant His6- and myc-tagged Geminin (myc-Geminin). Mobility-shifted Geminin bands were detected in the reaction products (Fig. S8*B*). Intensity of the bands increased and mobility also shifted according to dosage of the RDCOXB4 complex and the reaction time. Next, an in vitro ubiquitination assay with biotin-tagged ubiquitin (biotin-ubiquitin) was performed to determine whether the shifted bands corresponded with ubiquitinated Geminin (Fig. 5*B*). myc-Geminin was then immunoprecipitated with an anti-myc polyclonal antibody after the reaction, and similar mobility-shifted bands were detected in the immunoprecipitate through biotin–avidin interaction, confirming that the mobility-shifted bands represented ubiquitinated Geminin. The lower two mobility-shifted bands (Fig. S8*C*) were detectable in the reaction products obtained with methyl-ubiquitin, whereas more mobility-shifted bands were not, indicating that the former corresponded to mono-ubiquitinated Geminin and the latter to Geminin with more elongated ubiquitin chains.

Hoxb4N>A tended to form the RDCOXB4 complex more efficiently and/or stably than did wild-type Hoxb4 (Fig. 5*A*). The poly-ubiquitination activity was, however, abrogated by a single amino acid substitution (Fig. 5*C*), suggesting that the E3 ubiquitin ligase activity for Geminin of RDCOXB4 was mediated by a homeodomain in Hoxb4, which provides an interaction domain with Geminin. These findings clearly showed in vitro that Hoxb4 formed the RDCOXB4 complex and acted as the E3 ubiquitin ligase for Geminin. We also compared E3 ubiquitin ligase activities in GST-Roc1, RDOXB4(-Cul4a), RDC(-Hoxb4), RCOXB4 (-Ddb1), and RDCOXB4 (Fig. 5 *A* and *C*). The mobility-shifted bands for poly-ubiquitinated Geminin were undetectable in GST-Roc1, RDOXB4(-Cul4a), RDC(-Hoxb4), and RCOXB4(-Ddb1) although those for mono-ubiquitinated Geminin were detectable (Fig. 5*C*). Even in the absence of either Cul4a or Ddb1, GST-Roc1 interacted with Hoxb4 but displayed mono-ubiquitination activity only for Geminin (Fig. 5*C*). Each of the RDCOXB4 members may thus be required for an effective induction of poly-ubiquitination. To eliminate the possibility that Geminin was ubiquitinated by contaminated APC/C, we confirmed that a similar activity occurred in Geminin-DBD (Fig. S8*D*). We also examined ubiquitination of each of the RDCOXB4 members in the reaction products. The RDCOXB4 complex itself may thus also be subjected to self-ubiquitination (Fig. S8*E*).

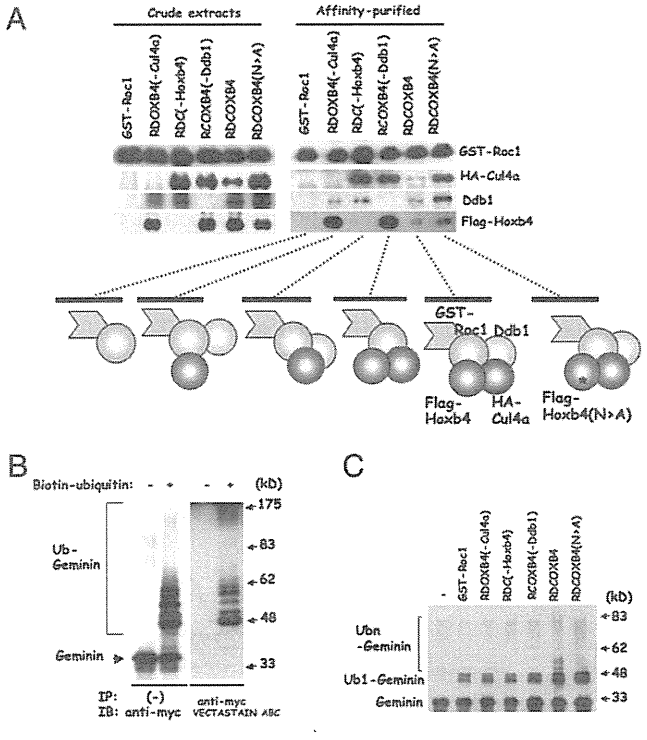

Fig. 5. Reconstitution and purification of the RDCOXB4 complex in Sf9 and E3 ubiquitin ligase activity for Geminin. (*A*) Crude extracts: expression of each member of the complex was detected in crude extracts by immunoblot analysis. Affinity-purified: pull-down assay of the complex with GST-Roc1. (*Lower*) Schematic representation of the complex. *, N>A mutation in the homeodomain of Hoxb4. (*B* and *C*) E3 ubiquitin ligase activity for Geminin. The affinity-purified recombinant complex was subjected to in vitro ubiquitination reaction (myc-Geminin + E1 + E2 + ubiquitin). (*B*) Reaction with biotin-tagged ubiquitin. Ubiquitinated Geminin was detected through biotin–avidin interaction in immunoprecipitated myc-Geminin. (*C*) The E3 ubiquitin ligase activity for Geminin in GST-Roc1, RDOXB4(-Cul4a), RDC(-Hoxb4), RCOXB4(-Ddb1), RDCOXB4, and RDCOXB4 (N>A). The amount of GST-Roc1 in the complex was adjusted to that of RDCOXB4 (1 μg).

Effect of Hoxb4 Transduction on E2F Activity and Its Target Gene Expression. Hoxb4 transduction increased mRNA for *Geminin*, *Cdt1*, and *Cyclin A2* in either Rae$^{+/+}$FLC or Rae$^{-/-}$FLC, whereas Hoxb4N>A did so less efficiently (Fig. S2*E*). Because these genes are under the regulation of E2F (28, 29), the induction was presumed to be mediated by E2F activation. We next examined the effect of Hoxb4 on E2F activity by means of a transient transfection experiment with an E2F-firefly luciferase reporter plasmid, pE2WTx4-Luc, in HEK-293 (Fig. 6*A*) (30). Hoxb4 overexpression induced luciferase activity in a dosage-dependent manner, but that of Hoxb4N>A did so less efficiently (Fig. 6*A*). Because Hoxb4 transfection reduced Geminin protein through UPS as mentioned above, we examined the effect of Geminin on E2F activity (Fig. 6*A*). siRNA-mediated knockdown of Geminin-induced E2F activity and restoration of reduced Geminin by 6myc-tagged Geminin transfection significantly reversed the effect, suggesting that Hoxb4 induced E2F activity at least in part through the direct regulation of Geminin.

Effect of Hoxb4 Transduction on Cdt1 and Mcm2. Finally, we examined by immunoblot analysis the effect of Hoxb4 on Cdt1 in the whole extract (Fig. S2*F*) as well as in the chromatin fraction (Fig. 6*B*). Transduction of Hoxb4 increased Cdt1 in the whole extract (Fig. S2*F*), probably through the aforementioned E2F activation, whereas that of Hoxb4N>A increased less efficiently. Similar induction was observed in Cyclin A2 (Fig. S2*F*) and Mcm2 (Fig. 6*B*). Hoxb4 transduction more prominently increased Cdt1 and Mcm2 in the chromatin fraction of Rae$^{-/-}$FLC (Fig. 6*B*), in which chromatin-loaded Cdt1 and Mcm2 were markedly reduced by accumulated Geminin as described previously (20). The down-regulation of Geminin protein was thus presumed to increase chromatin-loaded Cdt1 and Mcm2 either by E2F activation or by relieving the Geminin-mediated direct inhibition of Cdt1, promoting the prereplicative complex formation on chromatin to provide cells with higher proliferation potential.

Discussion

We show here that Hoxb4 directly interacts with Geminin through the homeodomain. Hoxb4 transduction induced formation of the RDCOXB4 complex, which may act as the E3 ubiquitin ligase for Geminin, whereas Hoxb4N>A constituted a similar complex that displayed little of the E3 ubiquitin ligase activity. Although the homeodomain of Hox proteins has long been believed to function as a DNA-binding domain (7), these findings indicate that the homeodomain may provide the RDCOXB4 complex with a recognition domain for Geminin. The involvement of the Roc1-Ddb1-Cul4a ubiquitin ligase core component in sustaining HSC activity is further supported by recently reported

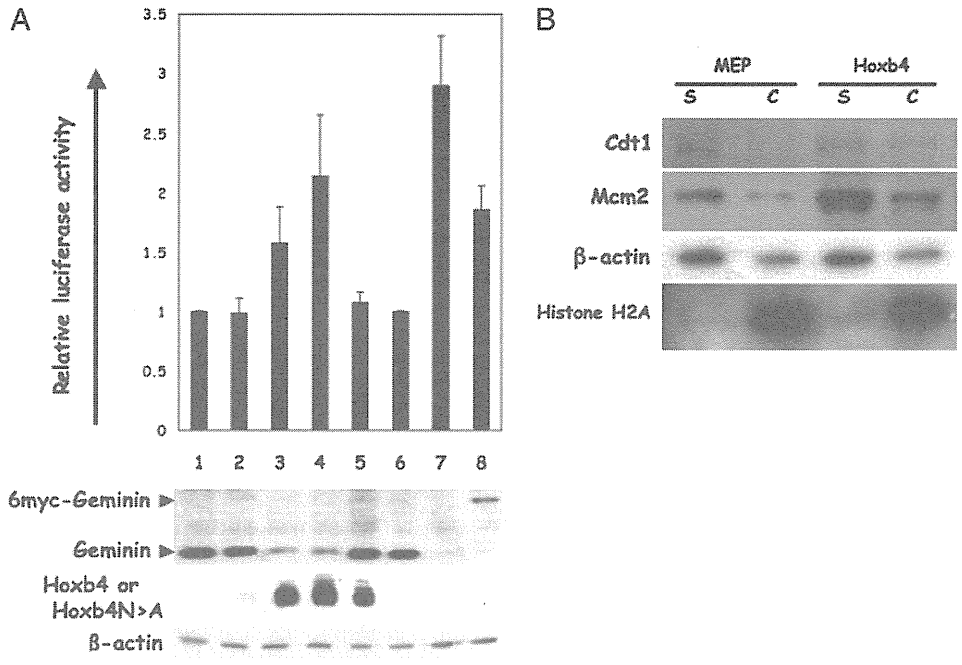

Fig. 6. Effect of Hoxb4 on E2F activity and DNA replication licensing. (*A*) Effect of Hoxb4 transfection on E2F activity. Renilla luciferase reporter plasmid driven by the mutant E2F-binding site, pE2MTx4-R, was used as control. (*Upper*) Firefly luciferase activity relative to that in mock vector-transfected cells. 1, mock vector; 2, Hoxb4—0.1 μg; 3, Hoxb4—0.5 μg; 4, Hoxb4—1 μg; 5, Hoxb4N>A—1 μg; 6, control siRNA; 7, siRNA for Geminin and a mock vector; 8, siRNA for Geminin and 6myc-tagged Geminin (0.1 μg). (*Lower*) Immunoblot analysis. (*B*) Effect of Hoxb4 transduction on Cdt1 and Mcm2 in the chromatin fraction of $Rae^{-/-}$FLC. S, soluble fraction; C, chromatin fraction. β-Actin and histone H2A were detected as control to ensure equal amounts of protein and purity of the chromatin fraction, respectively.

genetic evidence that the self-renewal and repopulating capacities, as well as hematopoietic differentiation, were impaired by *Cul4a* haploinsufficiency (24), although many target molecules for the Roc1-Ddb1-Cul4a component were reported. Hoxb4 transduction may down-regulate Geminin protein through UPS to relieve the inhibition of Cdt1, and down-regulated Geminin protein may also give rise to E2F activation, which facilitates loading of a DNA prereplicative complex onto chromatin to promote cell cycling. Because E2F activity was reported to be induced by Hoxb4 through the induction of c-Myc as mentioned above (9), Hoxb4 might induce E2F activity through either down-regulation of Geminin or up-regulation of c-Myc. Although it remains elusive in our study how down-regulated Geminin induces the E2F activation, the above findings suggest that Geminin by itself negatively regulates the transcription activity of its own promoter because transcription of *Geminin* is under the regulation of E2F (29). This may imply that a feedback mechanism plays a role in maintaining homeostasis of Geminin expression in cells. Hoxb4 transduction may thus affect Geminin homeostasis directly and indirectly, i.e., via the ubiquitination of Geminin and also via its effect on the transcription of *Geminin* to induce the HSC activity.

Although further detailed analysis is required, we propose a tentative model for the molecular mechanism showing how transduced Hoxb4 provides hematopoietic stem and progenitor cells with high proliferation potential on the basis of the findings in our current study (Fig. 7). Transduced Hoxb4 induces UPS-mediated down-regulation of Geminin protein by constituting the RDCOXB4 complex, an E3 ubiquitin ligase for Geminin, which results in augmentation of a prereplicative complex loaded onto chromatin as well as in transcription induction of the E2F target genes involved in DNA replication and cell cycling. The augmented prereplicative complex loaded onto chromatin may provide higher proliferation potential for hematopoietic stem and progenitor cells. As we previously reported, Geminin is highly expressed in $CD34^{-}KSL$ but is down-regulated in $CD34^{+}KSL$, progenitors, and their progeny subpopulations, whereas Cdt1 expression is reciprocal to Geminin expression (20). Thus, high Geminin expression is presumed to induce $CD34^{-}KSL$ to maintain quiescence and undifferentiated states through direct interaction with Cdt1(19) and Brg1/Brahma (21), respectively, whereas down-regulated Geminin may induce cellular proliferation and differentiation in the progeny subpopulations. Although the higher cellular proliferation potential might also help to induce self-renewal of HSCs, the precise molecular role for Geminin in Hoxb4 transduction-induced self-renewal activation of HSCs remains in-

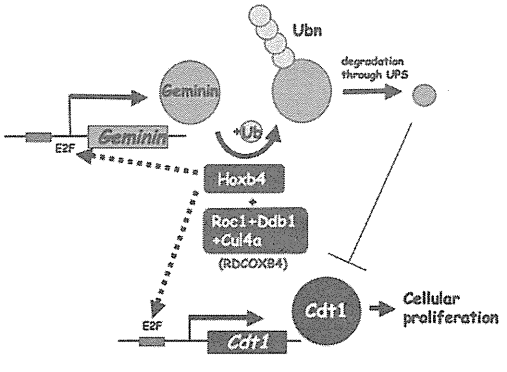

Fig. 7. Proposed tentative model for the molecular role of Hoxb4 in providing cells with proliferation potential. The pathway either enhanced or diminished by Hoxb4 transduction is indicated by thick and thin lines, respectively. Dotted lines indicated an indirect effect. E2F, E2F-binding site; Ub, ubiquitin.

sufficiently understood. Further detailed analysis of Geminin could provide an important clue for elucidating a molecular mechanism that sustains the hematopoietic stem and progenitor cell activity.

Materials and Methods

Animal experiments were done with C57BL6 mice and mice deficient in *Rae28* with a congenic genetic background. Plasmids and double-stranded RNAs (Dharmacon-ThermoFisher) were transfected by the calcium phosphate coprecipitation method and by using Lipofectamine RNAiMAX (Invitrogen-Life Technologies). Retrovirus-mediated gene transduction was performed with murine stem cell virus vectors. Hematopoiesis was assessed through clonogenic, LTC-IC, and LTR activities. The recombinant RDCOXB4 complexes were purified from Sf9 transfected with the baculovirus vectors and subjected to the in vitro ubiquitination assay. The statistically analyzed results are shown with SEM. A detailed description of all of the methods and antibodies used appear in *SI Materials and Methods* and in Table S1, respectively.

ACKNOWLEDGMENTS. We thank Drs. R. K. Humphries (University of British Columbia, Vancouver) and M. Kyba (University of Minnesota, Minneapolis) for providing the Hoxb4 cDNA; Dr. A. Kikuchi (Osaka University, Suita) for providing the pV-IKS and pVL1392 vectors; Dr. T. Inaba (Hiroshima University, Hiroshima) for the 32D cell line; the Analysis Center of Life Science in Hiroshima University, Ms. R. Tokimoto, and Y. Nakashima for technical assistance; Dr. M. Kanno (Hiroshima University, Hiroshima) for supporting Y.O., and Ms. A. Harada and H. Shimamoto for secretarial assistance. This work was supported by Grants-in-Aid for Scientific Research from the Ministry of Education, Culture, Sports, Science and Technology of Japan and by the Uehara Memorial Foundation, the Yamanouchi Foundation for Research on Metabolic Disorders, the Japan Leukaemia Research Fund, the Mitsubishi Pharma Research Foundation, the Novartis Foundation for the Promotion of Science, the Daiwa Securities Health Foundation, and the UBE Foundation.

1. Sauvageau G, et al. (1995) Overexpression of *HOXB4* in hematopoietic cells causes the selective expansion of more primitive populations in vitro and in vivo. *Genes Dev* 9: 1753–1765.
2. Antonchuk J, Sauvageau G, Humphries RK (2002) HOXB4-induced expansion of adult hematopoietic stem cells ex vivo. *Cell* 109:39–45.
3. Buske C, et al. (2002) Deregulated expression of HOXB4 enhances the primitive growth activity of human hematopoietic cells. *Blood* 100:862–868.
4. Kyba M, Perlingeiro RC, Daley GQ (2002) HoxB4 confers definitive lymphoid-myeloid engraftment potential on embryonic stem cell and yolk sac hematopoietic progenitors. *Cell* 109:29–37.
5. Amsellem S, et al. (2003) Ex vivo expansion of human hematopoietic stem cells by direct delivery of the HOXB4 homeoprotein. *Nat Med* 9:1423–1427.
6. Krosl J, et al. (2003) In vitro expansion of hematopoietic stem cells by recombinant TAT-HOXB4 protein. *Nat Med* 9:1428–1432.
7. McGinnis W, Krumlauf R (1992) Homeobox genes and axial patterning. *Cell* 68: 283–302.
8. Beslu N, et al. (2004) Molecular interactions involved in HOXB4-induced activation of HSC self-renewal. *Blood* 104:2307–2314.
9. Satoh Y, et al. (2004) Roles for c-Myc in self-renewal of hematopoietic stem cells. *J Biol Chem* 279:24986–24993.
10. Schiedlmeier B, et al. (2007) HOXB4's road map to stem cell expansion. *Proc Natl Acad Sci USA* 104:16952–16957.
11. Ohta H, et al. (2002) Polycomb group gene rae28 is required for sustaining activity of hematopoietic stem cells. *J Exp Med* 195:759–770.
12. Park IK, et al. (2003) Bmi-1 is required for maintenance of adult self-renewing haematopoietic stem cells. *Nature* 423:302–305.
13. Wang H, et al. (2004) Role of histone H2A ubiquitination in Polycomb silencing. *Nature* 431:873–878.
14. Takihara Y, et al. (1997) Targeted disruption of the mouse homologue of the *Drosophila polyhomeotic* gene leads to altered anteroposterior patterning and neural crest defects. *Development* 124:3673–3682.
15. Bracken AP, et al. (2007) The Polycomb group proteins bind throughout the INK4A-ARF locus and are disassociated in senescent cells. *Genes Dev* 21:525–530.
16. Chagraoui J, et al. (2006) E4F1: A novel candidate factor for mediating BMI1 function in primitive hematopoietic cells. *Genes Dev* 20:2110–2120.
17. Pomerantz J, et al. (1998) The Ink4a tumor suppressor gene product, p19Arf, interacts with MDM2 and neutralizes MDM2's inhibition of p53. *Cell* 92:713–723.
18. Le Cam L, et al. (2006) E4F1 is an atypical ubiquitin ligase that modulates p53 effector functions independently of degradation. *Cell* 127:775–788.
19. Blow JJ, Hodgson B (2002) Replication licensing: Defining the proliferative state? *Trends Cell Biol* 12:72–78.
20. Ohtsubo M, et al. (2008) Polycomb-group complex 1 acts as an E3 ubiquitin ligase for Geminin to sustain hematopoietic stem cell activity. *Proc Natl Acad Sci USA* 105: 10396–10401.
21. Seo S, et al. (2005) Geminin regulates neuronal differentiation by antagonizing Brg1 activity. *Genes Dev* 19:1723–1734.
22. Luo L, Yang X, Takihara Y, Knoetgen H, Kessel M (2004) The cell-cycle regulator geminin inhibits Hox function through direct and polycomb-mediated interactions. *Nature* 427:749–753.
23. Kim MY, et al. (2006) A repressor complex, AP4 transcription factor and geminin, negatively regulates expression of target genes in nonneuronal cells. *Proc Natl Acad Sci USA* 103:13074–13079.
24. Li B, et al. (2007) Cul4A is required for hematopoietic stem-cell engraftment and self-renewal. *Blood* 110:2704–2707.
25. Zhang Y, et al. (2003) CUL-4A stimulates ubiquitylation and degradation of the HOXA9 homeodomain protein. *EMBO J* 22:6057–6067.
26. McGarry TJ, Kirschner MW (1998) Geminin, an inhibitor of DNA replication, is degraded during mitosis. *Cell* 93:1043–1053.
27. Ohta T, Michel JJ, Schottelius AJ, Xiong Y (1999) ROC1, a homolog of APC11, represents a family of cullin partners with an associated ubiquitin ligase activity. *Mol Cell* 3:535–541.
28. Schulze A, et al. (1995) Cell cycle regulation of the cyclin A gene promoter is mediated by a variant E2F site. *Proc Natl Acad Sci USA* 92:11264–11268.
29. Yoshida K, Inoue I (2004) Regulation of Geminin and Cdt1 expression by E2F transcription factors. *Oncogene* 23:3802–3812.
30. Ohtani K, et al. (2000) Cell type-specific E2F activation and cell cycle progression induced by the oncogene product Tax of human T-cell leukemia virus type I. *J Biol Chem* 275:11154–11163.

Rapid Emergence of Telaprevir Resistant Hepatitis C Virus Strain from Wildtype Clone *In Vivo*

Nobuhiko Hiraga,[1,2] Michio Imamura,[1,2] Hiromi Abe,[1,2] C. Nelson Hayes,[1,2] Tomohiko Kono,[1,2] Mayu Onishi,[1,2] Masataka Tsuge,[1,2] Shoichi Takahashi,[1,2] Hidenori Ochi,[2,3] Eiji Iwao,[4] Naohiro Kamiya,[4] Ichimaro Yamada,[4] Chise Tateno,[2,5] Katsutoshi Yoshizato,[2,5] Hirotaka Matsui,[6] Akinori Kanai,[7] Toshiya Inaba,[6] Shinji Tanaka,[1,2] and Kazuaki Chayama[1,2,3]

Telaprevir is a potent inhibitor of hepatitis C virus (HCV) NS3-4A protease. However, the emergence of drug-resistant strains during therapy is a serious problem, and the susceptibility of resistant strains to interferon (IFN), as well as the details of the emergence of mutant strains *in vivo*, is not known. We previously established an infectious model of HCV using human hepatocyte chimeric mice. Using this system we investigated the biological properties and mode of emergence of mutants by ultra-deep sequencing technology. Chimeric mice were injected with serum samples obtained from a patient who had developed viral breakthrough during telaprevir monotherapy with strong selection for resistance mutations (A156F [92.6%]). Mice infected with the resistant strain (A156F [99.9%]) developed only low-level viremia and the virus was successfully eliminated with interferon therapy. As observed in patients, telaprevir monotherapy in viremic mice resulted in breakthrough, with selection for mutations that confer resistance to telaprevir (e.g., a high frequency of V36A [52.2%]). Mice were injected intrahepatically with HCV genotype 1b clone KT-9 with or without an introduced resistance mutation, A156S, in the NS3 region, and treated with telaprevir. Mice infected with the A156S strain developed lower-level viremia compared to the wildtype strain but showed strong resistance to telaprevir treatment. Although mice injected with wildtype HCV showed a rapid decline in viremia at the beginning of therapy, a high frequency (11%) of telaprevir-resistant NS3 V36A variants emerged 2 weeks after the start of treatment. *Conclusion:* Using deep sequencing technology and a genetically engineered HCV infection system, we showed that the rapid emergence of telaprevir-resistant HCV was induced by mutation from the wildtype strain of HCV *in vivo*. (HEPATOLOGY 2011;54:781-788)

Chronic hepatitis C virus (HCV) infection is a leading cause of cirrhosis, liver failure, and hepatocellular carcinoma.[1,2] The current standard treatment for patients chronically infected with HCV is the combination of peg-interferon (PEG-IFN) and ribavirin (RBV).[3-5] However, this treatment results in sustained viral response (SVR), defined as negative for HCV RNA 24 weeks after cessation of the therapy, in only about 50% of patients with genotype 1 HCV infection with high viral loads.[3-5] Given the low

Abbreviations: HCV, hepatitis C virus; HSA, human serum albumin; PEG-IFN, peg-interferon; RBV, ribavirin; RT-PCR, reverse transcript-polymerase chain reaction; SCID, severe combined immunodeficiency; SVR, sustained viral response; uPA, urokinase-type plasminogen activator.

From the [1]Department of Medicine and Molecular Science, Division of Frontier Medical Science, Programs for Biomedical Research, Graduate School of Biomedical Sciences, Hiroshima University, Hiroshima, Japan; [2]Liver Research Project Center, Hiroshima University, Hiroshima, Japan; [3]Laboratory for Digestive Diseases, RIKEN Center for Genomic Medicine, Hiroshima, Japan; [4]Research and Development Unit, Mitsubishi Tanabe Pharma Corp., Yokohama, Japan; [5]PhoenixBio Co., Ltd., Higashihiroshima, Japan; [6]Department of Molecular Oncology and Leukemia Program Project, Research Institute for Radiation Biology and Medicine, Hiroshima University, Hiroshima, Japan; [7]Radiation Research Center for Frontier Science, Research Institute for Radiation Biology and Medicine, Hiroshima University, Hiroshima, Japan.

Received January 17, 2011; accepted May 16, 2011.

Supported in part by a grant-in-aid for Scientific Research from the Japanese Ministry of Labor, Health and Welfare

Address reprint requests to: Prof. Kazuaki Chayama, M.D., Ph.D., Department of Medical and Molecular Science, Division of Frontier Medical Science, Programs for Biomedical Research, Graduate School of Biomedical Science, Hiroshima University, 1-2-3 Kasumi, Minami-ku, Hiroshima 734-8551, Japan. E-mail: chayama@hiroshima-u.ac.jp; fax: +81-82-255-6220.

View this article online at wileyonlinelibrary.com.

DOI 10.1002/hep.24460

Potential conflict of interest: E.I., N.K., I.Y. are employees of Mitsubishi Tanabe Pharma Corp. The other authors have nothing to declare.

effectiveness of the current therapy, many molecules have been screened for antiviral activity against HCV for use in development of novel anti-HCV therapies. A number of new selective inhibitors of HCV proteins, the so-called STAT-C (specifically targeted antiviral therapy for HCV) inhibitors, are currently under development. Telaprevir is a reversible, selective, specific inhibitor of the HCV NS3-4A protease that has shown potent antiviral activity in HCV replicon assays.[6] Although the antiviral effect of telaprevir is quite potent, monotherapy using these drugs results in rapid emergence of drug-resistant strains.[7,8] Accordingly, these drugs are used in combination with pegylated-IFN and ribavirin for chronic hepatitis C patients. Because the HCV virus replicates rapidly and RNA polymerase lacks a proofreading system, HCV viral quasispecies can emerge *de novo*, and some of these variants may confer resistance. Although a resistant variant is initially present at low frequency, it may quickly emerge as the dominant species during antiviral treatment.[9,10] Resistant clones against HCV NS3-4A protease inhibitors have reportedly been induced in replicon systems.

The immunodeficient urokinase-type plasminogen activator (uPA) mouse permits repopulation of the liver with human hepatocytes, resulting in human hepatocyte chimeric mice that are able to develop HCV viremia after injection of serum samples positive for the virus.[11] We and other groups have reported that the human hepatocyte chimeric mouse is useful for evaluating the effect of NS3-4A protease inhibitor.[12,13] Using this mouse model, we developed a reverse genetics systems for HCV.[14,15] This system is useful to study characteristics of HCV strains with various substitutions of interest because the confounding effects of quasispecies can be minimized. Using ultra-deep sequencing technology, we demonstrate the rapid emergence of telaprevir resistance in HCV as a result of mutation from wildtype strain using genetically engineered HCV-infected human hepatocyte chimeric mice.

Materials and Methods

Animal Treatment. Generation of the uPA$^{+/+}$/SCID$^{+/+}$ mice and transplantation of human hepatocytes were performed as described recently by our group.[16] All mice were transplanted with frozen human hepatocytes obtained from the same donor. Mice received humane care and all animal protocols were performed in accordance with the guidelines of the local committee for animal experiments. Infection, extraction of serum samples, and sacrifice were performed under ether anesthesia. Mice were injected either intravenously with HCV-positive human serum samples or intrahepatically with *in vitro*-transcribed genotype 1b HCV RNA. HCV-infected mice were administered either perorally with 200-300 mg/kg of telaprevir (VX950; MP424; Mitsubishi Tanabe Pharma, Osaka, Japan) twice a day or intramuscularly with 1,500 IU/g of IFN-alpha (Dainippon Sumitomo Pharma, Tokyo). The telaprevir dose was determined in a previous study in which this dosage range was found to yield serum concentrations equivalent to treated human patients.[13]

Human Serum Samples. After obtaining written informed consent, human serum samples containing genotype 1b HCV were obtained from two patients with chronic hepatitis. The individual serum samples were divided into aliquots and stored separately in liquid nitrogen until use. The study protocol conforms to the ethical guidelines of the 1975 Declaration of Helsinki and was approved *a priori* by the Institutional Review Committee.

HCV RNA Transcription and Inoculation into Chimeric Mice. We have previously established an infectious genotype 1b HCV clone HCV-KT9 derived from a Japanese patient with severe acute hepatitis (GenBank access. no. AB435162).[15] We cloned this HCV complementary DNA (cDNA) into plasmid pBR322 under a T7 RNA promoter to create the plasmid pHCV-KT9. Ten μg of plasmid DNA, linearized by *Xba*I (Promega, Madison, WI) digestion, were transcribed in a 100 μL reaction volume with T7 RNA polymerase (Promega) at 37°C for 2 hours and analyzed by agarose gel electrophoresis. Each transcription mixture was diluted with 400 μL of phosphate-buffered saline (PBS) and injected into the livers of chimeric mice.[15] The QuikChange site-directed mutagenesis kit (Stratagene, Foster City, CA) was used to introduce a substitution at amino acid 156 of the NS3 region (A156S).

RNA Extraction and Amplification. RNA was extracted from serum samples by Sepa Gene RV-R (Sankojunyaku, Tokyo), dissolved in 8.8 μL RNase-free H_2O, and reverse transcribed using a random primer (Takara Bio, Shiga, Japan) and M-MLV reverse transcriptase (ReverTra Ace, Toyobo, Osaka, Japan) in a 20-μL reaction mixture according to the instructions provided by the manufacturer. Nested polymerase chain reaction (PCR) and quantitation of HCV by Light Cycler (Roche Diagnostic, Japan, Tokyo) were performed as reported.[15]

Ultra-Deep Sequencing. We adapted multiplex sequencing-by-synthesis to simultaneously sequence

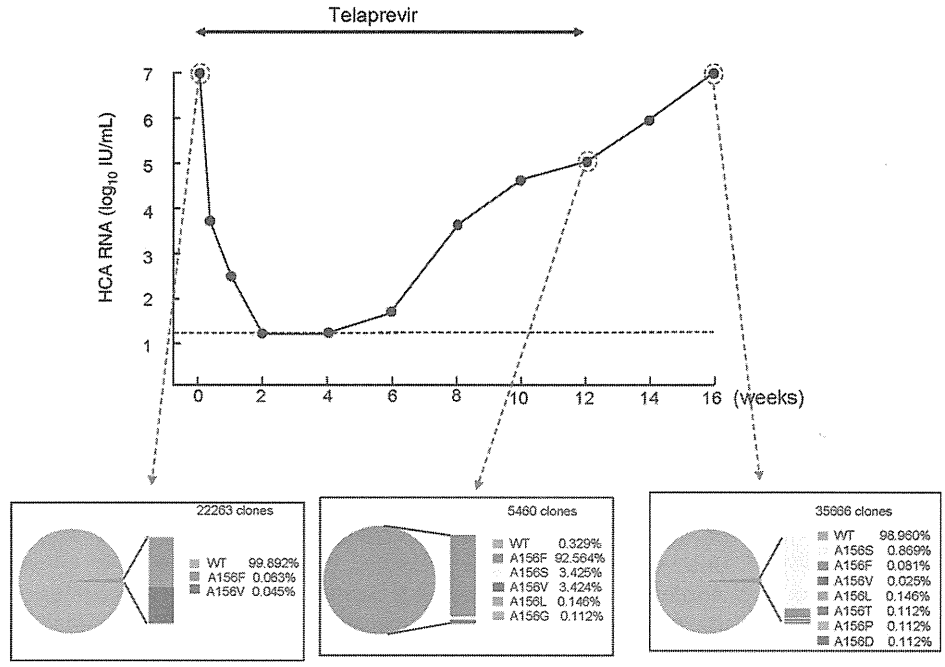

Fig. 1. Changes in serum HCV RNA levels in a telaprevir-treated chronic hepatitis C patient. A 55-year-old woman infected with genotype 1b HCV was treated with 750 mg of telaprevir every 8 hours for 12 weeks. Serum HCV RNA (upper panel) and the amino acid (aa) frequencies at aa156 in the HCV NS3 region by ultra-deep sequencing at the indicated times are shown. The horizontal dotted line indicates the detectable limit (1.2 log copy/mL).

multiple genomes using the Illumina Genome Analyzer. Briefly, cDNA was fragmented using sonication and the resultant fragment distribution was assessed using the Agilent BioAnalyzer 2100 platform. A library was prepared using the Multiplexing Sample Preparation Kit (Illumina, CA). Imaging analysis and base calling were performed using Illumina Pipeline software with default settings.[17-23] The N-terminal 543 nucleotides of NS3 protease were analyzed. This technique revealed an average coverage depth of over 1,000 sequence reads per basepair in the unique regions of the genome. Read mapping to a reference sequence was performed using Bowtie.[24] Because of the short 36 nucleotide read length, mapping hypervariable regions with multiple closely spaced variants against a reference sequence yields poor coverage. Therefore, common variants were identified by relaxing the mismatch settings as well as using *de novo* assembly using ABySS.[25] Multiple alternative reference sequences were included to improve coverage in variable regions. Codon counts were merged and analyzed using R v. 2.12.

Results

Emergence of a Telaprevir-Resistant Variant in a Hepatitis C Patient Treated with Telaprevir and Analysis of the A156F Mutation. A 55-year-old woman infected with genotype 1b HCV was treated with 750 mg of telaprevir every 8 hours for 12 weeks (Fig. 1). After 1 weeks of treatment, serum HCV RNA titer decreased below the detectable limit (1.2 log copy/mL). However, HCV RNA titer became positive by week 4. By week 12, HCV RNA titer had increased to 4.8 log copy/mL and telaprevir treatment was discontinued. Because direct sequence analysis showed an A156F mutation in the NS3 region in the serum samples at 12 weeks, we performed ultra-deep sequence analysis and confirmed the high frequency (92.5%) of A156F mutation. Four weeks after cessation of treatment (at 16 weeks), sequence analysis revealed that the major strain had reverted to wildtype (99%). To analyze the replication ability and the susceptibility of the A156F mutation to telaprevir, 100 μL serum samples containing 10^4 copies of HCV obtained at week 12 were injected into human hepatocyte chimeric mice. Two wildtype HCV-inoculated mice became positive for HCV RNA 2 weeks after inoculation and serum HCV RNA titer increased to high levels (7.6 and 7.8 log copy/mL, respectively) at 6 weeks after inoculation (Fig. 2). In contrast to wildtype HCV-infected mice, a mouse inoculated with serum containing the A156F mutant developed measurable viremia at 4 weeks postinoculation, although serum HCV RNA titer remained low at 6 weeks (5.2 log copy/mL). Eight weeks after inoculation ultra-deep sequence analysis showed a high frequency (99.9%) of A156F mutation. From this point the mouse was administrated 200 mg/kg of telaprevir perorally twice a day for 4 weeks. However, this treatment resulted in no reduction in serum HCV RNA level. During the observation period the A156F mutation remained at

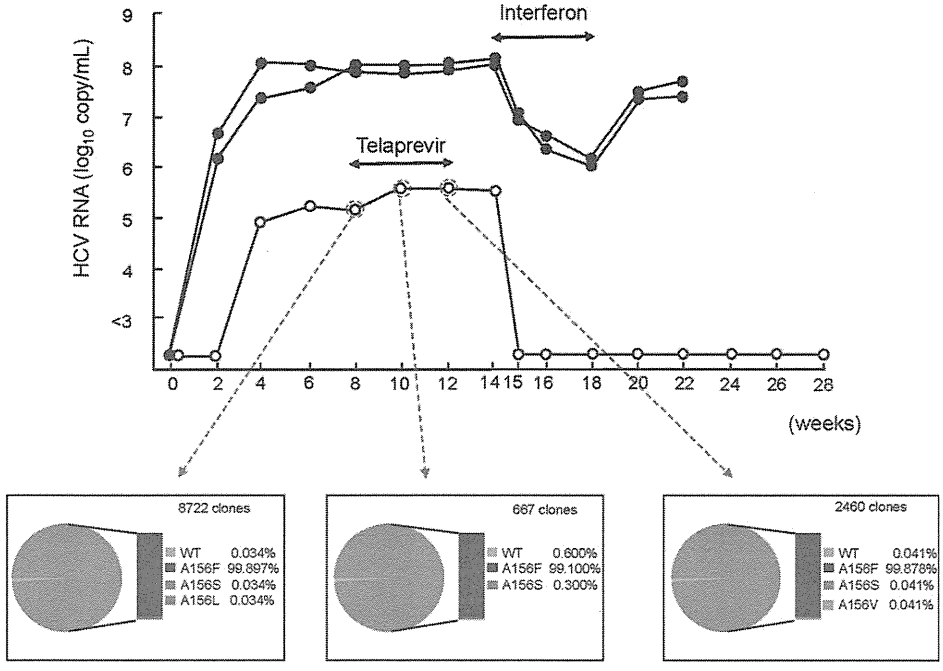

Fig. 2. Changes in serum virus titers in HCV-infected mice. Mice were injected with either wildtype (closed circles) or A156F-mutated HCV serum samples (obtained from an HCV-infected patient who received telaprevir monotherapy for 12 weeks; see Fig. 1) (open circles). Six weeks after injection the A156F mutant mouse was treated with 200 mg/kg of telaprevir orally twice a day for 4 weeks and injected intramuscularly with 1,500 IU/g/day of interferon-alpha for 4 weeks. Serum HCV RNA (upper panel) and amino acid (aa) frequencies at aa156 in the HCV NS3 region by ultra-deep sequencing at the indicated times are shown.

high frequency (>99%). To analyze the susceptibility of the A156F mutation to IFN, wildtype or A156F-mutated HCV-infected mice were treated with 1,500 IU/g/day of IFN-alpha for 4 weeks. Treatment resulted in only a two log reduction in HCV RNA level in wildtype HCV-infected mice. In contrast, serum HCV RNA titer decreased below the detectable limit 1 week after treatment in an A156F-infected mouse. Ten weeks after cessation of IFN-treatment (at week 28), HCV RNA in the mouse serum remained undetectable, suggesting that HCV RNA was eliminated. These results demonstrate that the A156F variant is associated with telaprevir-resistance, but the mutant has low replication ability and a high susceptibility to IFN.

Effect of Telaprevir on HCV-Infected Mice and Sequence Analysis of NS3 Region. Next we investigated the effect of telaprevir on wildtype HCV-infected mice. Two chimeric mice were inoculated intravenously with serum samples containing 10^5 copies of HCV obtained from an HCV-positive patient (Fig. 3). Six weeks after inoculation both mice were administered 200 mg/kg of telaprevir perorally twice a day for 4 weeks. Serum HCV RNA titer in both mice rapidly decreased; however, in one of the mice HCV RNA titer increased again 3 weeks after the start of treatment. Ultra-deep sequence analysis of the NS3 region showed that following the start of telaprevir administration the frequency of the V36A mutation increased from 18% at 2 weeks to 52% at 4 weeks, at which point it was accompanied by an increase in the HCV RNA titer. Two weeks after cessation of telaprevir treatment (at week 12), ultra-deep sequence analysis revealed that the frequency of the V36A mutant had decreased to 13% and the frequency of the wildtype HCV had increased to 84%, although the HCV RNA titer increased only slightly.

Intrahepatic Injection of HCV-KT9-Wild RNA and KT9-NS3-A156S RNA into Human Hepatocyte Chimeric Mice. We previously established an infectious genotype 1b HCV clone, HCV-KT9 (HCV-KT9-wild).[15] We created a telaprevir-resistant HCV clone by introducing an A156S amino acid substitution in the NS3 region of HCV-KT9 (KT9-NS3-A156S) (Fig. 4A). Using wildtype and telaprevir-resistant clones we investigated the replication ability *in vivo*. Mice were injected intrahepatically with 30 μg of *in vitro*-transcribed HCV-KT9-wild RNA or KT9-NS3-A156S RNA. Mice injected with HCV-KT9-wild developed measurable viremia at 2 weeks postinoculation and by 4 weeks postinoculation HCV RNA had reached 10^7 copy/mL (Fig. 4B). On the other hand, mice injected with KT9-NS3-A156S developed measurable viremia at 4 weeks postinoculation but maintained only low levels of viremia. These results suggest that the telaprevir-resistant HCV clone has a lowered replication ability compared to the wildtype HCV clone *in vivo*.

Treatment with Telaprevir and Analysis of Mutagenesis in Mice. Two mice infected with HCV-KT9-wild and one mouse infected with KT9-NS3-A156S were treated with 200 mg/kg of telaprevir twice a day for 2 weeks (Fig. 5A), resulting in 1.4 and 2.7 log

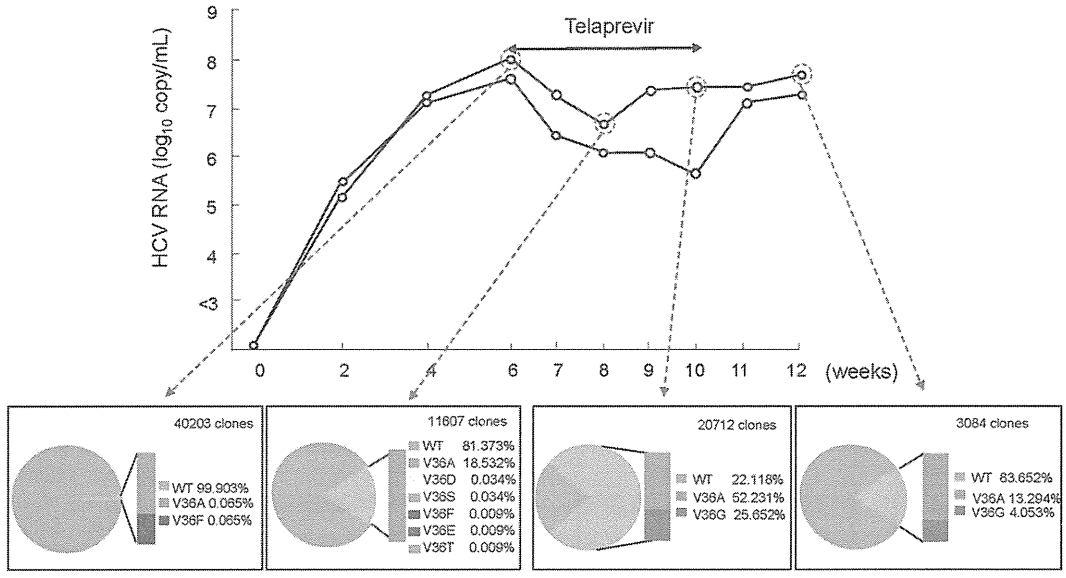

Fig. 3. Treatment with telaprevir in wildtype HCV-infected mice. Two mice were injected intravenously with 50 μL of HCV-positive human serum samples. Six weeks after HCV injection mice were treated with 200 mg/kg of telaprevir orally twice a day for 4 weeks. Serum HCV RNA (upper panel) and amino acid (aa) frequencies at aa36 in the HCV NS3 region by ultra-deep sequencing at the indicated times are shown.

reductions in HCV RNA level in the two wildtype HCV-infected mice. In contrast, only a 0.6 log reduction was observed in the KT9-NS3-A156S-infected mouse. These results demonstrate that our human hepatocyte chimeric mouse model infected with *in vitro*-transcribed HCV RNA provides an effective system for analysis of the susceptibility of HCV mutants to antiviral drugs. Interestingly, ultra-deep sequence analysis showed a rapid emergence of a V36A variant in the NS3 region in mouse serum 2 weeks after treatment (Fig. 5B). Four weeks after cessation of treatment (at week 6) the frequency of the V36A variant had decreased. Mice were then treated with 300 mg/kg of telaprevir twice a day for 4 weeks, which resulted in an elevated frequency of V36A variants at 1 (at week 7, 5.4%) and 4 weeks (at 10 week, 41.8%) after treatment and no reduction in serum HCV RNA level. These results suggest that telaprevir-resistant mutations emerged *de novo* from the wildtype strain of HCV, presumably through error-prone replication and potent selection for telaprevir escape mutants. During the telaprevir treatment period no increases of HCV RNA titers in these mice were observed, probably due to the low frequency of the resistant strain.

Discussion

Telaprevir is a peptidomimetic inhibitor of the NS3-4A serine protease that is currently undergoing clinical evaluation. Despite its effectiveness against HCV, some patients have shown a rapid viral breakthrough during the first 14 days of treatment.[26] Population sequencing of the viral NS3 region identified a number of mutations near the NS3 protease catalytic

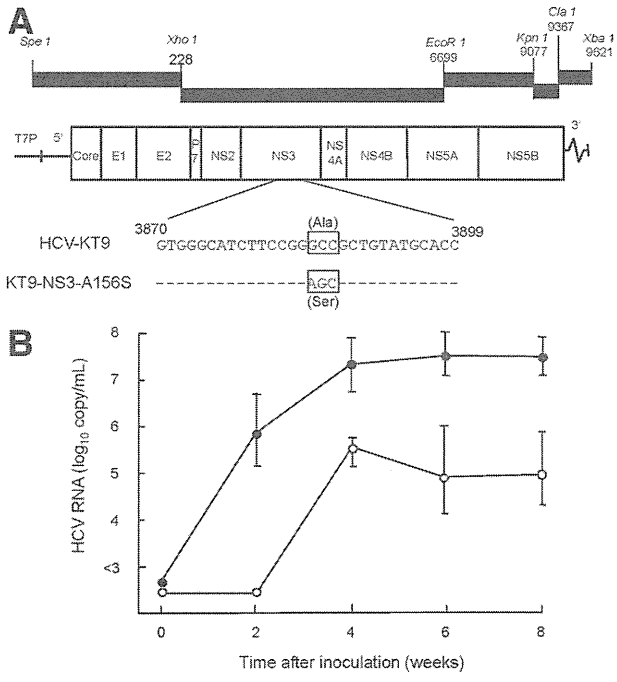

Fig. 4. Intrahepatic injection of *in vitro* transcribed HCV-KT9 RNA and KT9-NS3-A156S RNA into human hepatocyte chimeric mice. (A) The schematic of infectious genotype 1b HCV clones, HCV-KT9 and KT9-NS3-A156S. Boxes indicate codons at amino acid 156 in HCV NS3 region. Ala, alanine; Ser, serine. (B) Changes in serum levels of HCV RNA in mice intrahepatically injected with either HCV-KT9 RNA (closed circles) or KT9-NS3-A156S RNA (open circles). Data are represented as the mean ± SD of three mice.

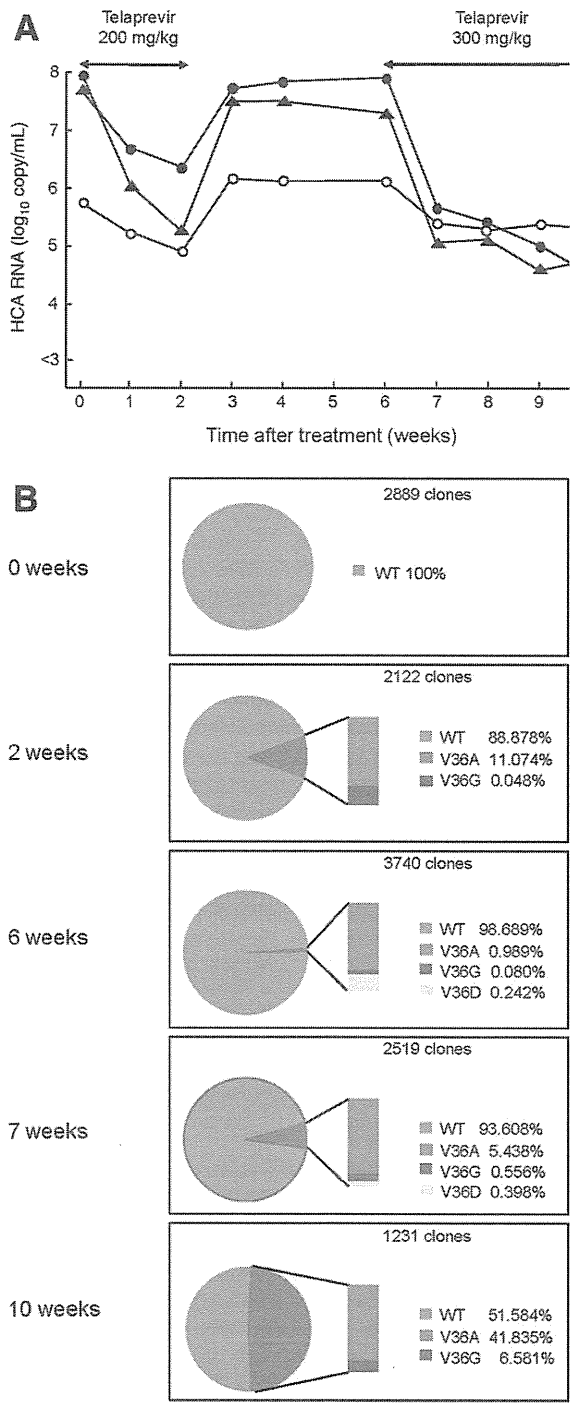

Fig. 5. The effect of telaprevir on mice infected with *in vitro*-transcribed HCV. Mice were injected with *in vitro*-transcribed HCV-KT9 RNA (closed circles and closed triangles) or KT9-NS3-A156S RNA (open circles). Six weeks after HCV RNA injection, mice were treated perorally with 200 mg/kg of telaprevir twice a day for 2 weeks. Four weeks after cessation of treatment mice were treated with 300 mg/kg of telaprevir twice a day for 4 weeks. (A) Mice serum HCV RNA titers at the indicated times are shown. Serum samples obtained from one of two HCV-KT9-infected mice (closed triangles) were used for ultra-deep sequencing. (B) Amino acid (aa) frequencies at aa36 in the HCV NS3 region based on ultra-deep sequencing are shown.

domain.[26] In particular, variants at NS3 residues 36, 54, 155, and 156 were shown to confer reduced sensitivity to telaprevir.[27]

In this study we analyzed the association between the antiviral efficacy of telaprevir and sequence variants within the NS3 region using chimeric mice infected with serum samples obtained from an HCV genotype 1b-infected patient. One of two HCV-infected mice had a viral breakthrough during the dosing period (Fig. 3). Ultra-deep sequence analysis of the NS3 region showed an increase of the V36A mutant, which has been reported to confer telaprevir resistance.[26] Consequently, our results show evidence of emergence of a telaprevir-resistant variant previously detected in human clinical trials.

We detected an A156F mutant in the HCV NS3 region in a chronic hepatitis patient who had experienced viral breakthrough during telaprevir monotherapy (Fig. 1). Likewise, HCV RNA titer in mice infected with the A156F variant showed no reduction following 2 weeks of telaprevir treatment (Fig. 2). However, 2 weeks of treatment with IFN-alpha rapidly suppressed serum HCV RNA titer below the detectable limit. These results demonstrate that A156F is telaprevir-resistant but has a high susceptibility to IFN.

Interestingly, ultra-deep sequencing revealed that the wildtype strain was present at low frequency (0.3%) in the serum inoculum (Fig. 2). However, the frequency of the wildtype failed to increase over time (Fig. 3), suggesting that the very small number of wildtype viral RNA (about 30 copies) may be incomplete or defective, as a large proportion of viral genomes are thought to be defective due to the virus's high replication and mutation rates.[9] Further analysis is necessary in order to interpret the significance of the presence of very low frequency variants detected by ultra-deep sequencing.

The short read lengths used in next generation sequencing also complicates the detection of rare variants, especially when variants are clustered within a region smaller than an individual read length (e.g., 36 basepairs). Relaxing the matching criteria allows mapping of more diverse reads but increases the error rate, whereas default settings may be geared toward more genetically homogenous haploid or diploid genomes. In this study we used *de novo* assembly to identify more diverse variants that failed to map to the reference sequence. Examining the variation in codon frequencies among samples, we created alternative reference sequences containing a sufficient range of variants to provide more uniform coverage of variable regions.

Using our previously established infectious HCV-KT9 genotype 1b HCV clone, we investigated the antiviral efficacy of telaprevir and the effect of

resistance mutations on viral replication. HCV RNA titer in mice infected with the telaprevir-resistant strain KT9-NS3-A156S was lower than in mice infected with the wildtype strain HCV-KT9-wild (Fig. 4B). HCV NS proteins include proteases for sequential processing of the polyprotein and are thought to be important in viral replication.[28] Our results suggest that differences in viral fitness underlie the differences in viral replication capacity. We analyzed the antiviral efficacy of telaprevir and the sequence of the NS3 region using HCV-infected mice treated with telaprevir. Although telaprevir treatment suppressed serum HCV RNA titer in mice infected with HCV-KT9, the decline of HCV RNA titer was only 0.6 log copy/mL in a mouse infected with KT9-NS3-A156S under the same treatment (Fig. 5A). These results suggest that our genetically engineered HCV-infected mouse model is useful for analyzing HCV escape mutants associated with antiviral drugs. Interestingly, treatment with telaprevir resulted in selection for V36A variants in the NS3 region in an HCV-KT9-infected mouse (Fig. 5B). There are a few controversial reports proposing that resistant variants may already be present at low frequency (<1%) within the quasispecies population in treatment-naïve patients,[29] consistent with their rapid emergence only days after treatment initiation.[26,30] This might well occur, due to the large number of mutated HCV clones. However, our results provide evidence in support of *de novo* emergence of telaprevir resistance induced by viral mutation followed by selection. HCV has both a high replication rate (10^{12} particles per day) and a high mutation rate (10^{-3} to 10^{-4}),[9,10] suggesting that the viral quasispecies population is likely to represent a large and genetically diverse substrate for immune selection.

In summary, we established an infection model of a genotype 1b HCV clone using the human hepatocyte chimeric mouse model. Using this model we demonstrate rapid emergence of *de novo* telaprevir-resistant HCV quasispecies from wildtype HCV.

Acknowledgment: The authors thank Rie Akiyama, Kazuyo Hattori, Yoshie Yoshida, Kiyomi Toyota, and Yoko Matsumoto for expert technical assistance.

References

1. Kiyosawa K, Sodeyama T, Tanaka E, Gibo Y, Yoshizawa K, Nakano Y, et al. Interrelationship of blood transfusion, non-A, non-B hepatitis and hepatocellular carcinoma: analysis by detection of antibody to hepatitis C virus. HEPATOLOGY 1990;12:671-675.
2. Niederau C, Lange S, Heintges T, Erhardt A, Buschkamp M, Hurter D, et al. Prognosis of chronic hepatitis C: results of a large, prospective cohort study. HEPATOLOGY 1998;28:1687-1695.
3. Manns MP, McHutchison JG, Gordon SC, Rustgi VK, Shiffman M, Reindollar R, et al. Peginterferon alfa-2b plus ribavirin compared with interferon alfa-2b plus ribavirin for initial treatment of chronic hepatitis C: a randomised trial. Lancet 2001;358:958-965.
4. Fried MW, Shiffman ML, Reddy KR, Smith C, Marinos G, Goncales FL Jr, et al. Peginterferon alfa-2a plus ribavirin for chronic hepatitis C virus infection. N Engl J Med 2002;347:975-982.
5. Hoofnagle JH, Ghany MG, Kleiner DE, Doo E, Heller T, Promrat K, et al. Maintenance therapy with ribavirin in patients with chronic hepatitis C who fail to respond to combination therapy with interferon alfa and ribavirin. HEPATOLOGY 2003;38:66-74.
6. Perni RB, Almquist SJ, Byrn RA, Chandorkar G, Chaturvedi PR, Courtney LF, et al. Preclinical profile of VX-950, a potent, selective, and orally bioavailable inhibitor of hepatitis C virus NS3–4A serine protease. Antimicrob Agents Chemother 2006;50:899-909.
7. Lin C, Gates CA, Rao BG, Brennan DL, Fulghum JR, Luong YP, et al. In vitro studies of cross-resistance mutations against two hepatitis C virus serine protease inhibitors, VX-950 and BILN 2061. J Biol Chem 2005;280:36784-36791.
8. Mo H, Lu L, Pilot-Matias T, Pithawalla R, Mondal R, Masse S, et al. Mutations conferring resistance to a hepatitis C virus (HCV) RNA-dependent RNA polymerase inhibitor alone or in combination with an HCV serine protease inhibitor in vitro. Antimicrob Agents Chemother 2005;49:4305-4314.
9. Bartenschlager R, Lohmann V. Replication of hepatitis C virus. J Gen Virol 2000;81:1631-1648.
10. Rong L, Dahari H, Ribeiro RM, Perelson AS. Rapid emergence of protease inhibitor resistance in hepatitis C virus. Sci Transl Med 2010;2:30ra32.
11. Mercer DF, Schiller DE, Elliott JF, Douglas DN, Hao C, Rinfret A, et al. Hepatitis C virus replication in mice with chimeric human livers. Nat Med 2001;7:927-933.
12. Kneteman NM, Weiner AJ, O'Connell J, Collett M, Gao T, Aukerman L, et al. Anti-HCV therapies in chimeric scid-Alb/uPA mice parallel outcomes in human clinical application. HEPATOLOGY 2006;43:1346-1353.
13. Kamiya N, Iwao E, Hiraga N, Tsuge M, Imamura M, Takahashi S, et al. Practical evaluation of a mouse with chimeric human liver model for hepatitis C virus infection using an NS3–4A protease inhibitor. J Gen Virol 2010;91:1668-1677.
14. Hiraga N, Imamura M, Tsuge M, Noguchi C, Takahashi S, Iwao E, et al. Infection of human hepatocyte chimeric mouse with genetically engineered hepatitis C virus and its susceptibility to interferon. FEBS Lett 2007;581:1983-1987.
15. Kimura T, Imamura M, Hiraga N, Hatakeyama T, Miki D, Noguchi C, et al. Establishment of an infectious genotype 1b hepatitis C virus clone in human hepatocyte chimeric mice. J Gen Virol 2008;89:2108-2113.
16. Tateno C, Yoshizane Y, Saito N, Kataoka M, Utoh R, Yamasaki C, et al. Near completely humanized liver in mice shows human-type metabolic responses to drugs. Am J Pathol 2004;165:901-912.
17. Cronn R, Liston A, Parks M, Gernandt DS, Shen R, Mockler T. Multiplex sequencing of plant chloroplast genomes using Solexa sequencing-by-synthesis technology. Nucleic Acids Res 2008;36:e122.
18. Mitsuya Y, Varghese V, Wang C, Liu TF, Holmes SP, Jayakumar P, et al. Minority human immunodeficiency virus type 1 variants in antiretroviral-naive persons with reverse transcriptase codon 215 revertant mutations. J Virol 2008;82:10747-10755.
19. Margeridon-Thermet S, Shulman NS, Ahmed A, Shahriar R, Liu T, Wang C, et al. Ultra-deep pyrosequencing of hepatitis B virus quasispecies from nucleoside and nucleotide reverse-transcriptase inhibitor (NRTI)-treated patients and NRTI-naive patients. J Infect Dis 2009;199:1275-1285.
20. Szpara ML, Parsons L, Enquist LW. Sequence variability in clinical and laboratory isolates of herpes simplex virus 1 reveals new mutations. J Virol 2010;84:5303-5313.

21. Wright CF, Morelli MJ, Thebaud G, Knowles NJ, Herzyk P, Paton DJ, et al. Beyond the consensus: dissecting within-host viral population diversity of foot-and-mouth disease virus by using next-generation genome sequencing. J Virol 2011;85:2266-2275.
22. Verbinnen T, Van Marck H, Vandenbroucke I, Vijgen L, Claes M, Lin TI, et al. Tracking the evolution of multiple in vitro hepatitis C virus replicon variants under protease inhibitor selection pressure by 454 deep sequencing. J Virol 2010;84:11124-11133.
23. Wang GP, Sherrill-Mix SA, Chang KM, Quince C, Bushman FD. Hepatitis C virus transmission bottlenecks analyzed by deep sequencing. J Virol 2010;84:6218-6228.
24. Langmead B, Trapnell C, Pop M, Salzberg SL. Ultrafast and memory-efficient alignment of short DNA sequences to the human genome. Genome Biol 2009;10:R25.
25. Simpson JT, Wong K, Jackman SD, Schein JE, Jones SJ, Birol I. ABySS: a parallel assembler for short read sequence data. Genome Res 2009;19:1117-1123.
26. Sarrazin C, Kieffer TL, Bartels D, Hanzelka B, Muh U, Welker M, et al. Dynamic hepatitis C virus genotypic and phenotypic changes in patients treated with the protease inhibitor telaprevir. Gastroenterology 2007;132:1767-1777.
27. Kuntzen T, Timm J, Berical A, Lennon N, Berlin AM, Young SK, et al. Naturally occurring dominant resistance mutations to hepatitis C virus protease and polymerase inhibitors in treatment-naive patients. HEPATOLOGY 2008;48:1769-1778.
28. Hijikata M, Mizushima H, Tanji Y, Komoda Y, Hirowatari Y, Akagi T, et al. Proteolytic processing and membrane association of putative nonstructural proteins of hepatitis C virus. Proc Natl Acad Sci U S A 1993;90:10773-10777.
29. Lu L, Mo H, Pilot-Matias TJ, Molla A. Evolution of resistant M414T mutants among hepatitis C virus replicon cells treated with polymerase inhibitor A-782759. Antimicrob Agents Chemother 2007;51:1889-1896.
30. Kieffer TL, Sarrazin C, Miller JS, Welker MW, Forestier N, Reesink HW, et al. Telaprevir and pegylated interferon-alpha-2a inhibit wild-type and resistant genotype 1 hepatitis C virus replication in patients. HEPATOLOGY 2007;46:631-639.

THE JOURNAL OF BIOLOGICAL CHEMISTRY VOL. 286, NO. 7, pp. 5589–5598, February 18, 2011

The Dynactin Complex Maintains the Integrity of Metaphasic Centrosomes to Ensure Transition to Anaphase*[S]

Received for publication, July 22, 2010, and in revised form, December 14, 2010 Published, JBC Papers in Press, December 16, 2010, DOI 10.1074/jbc.M110.167742

Yuko Ozaki, Hirotaka Matsui, Akiko Nagamachi, Hiroya Asou, Daisuke Aki, and Toshiya Inaba[1]

From the Department of Molecular Oncology and Leukemia Program Project, Research Institute for Radiation Biology and Medicine, Hiroshima University, Hiroshima 734-8553, Japan

The dynactin complex is required for activation of the dynein motor complex, which plays a critical role in various cell functions including mitosis. During metaphase, the dynein-dynactin complex removes spindle checkpoint proteins from kinetochores to facilitate the transition to anaphase. Three components ($p150^{Glued}$, dynamitin, and p24) compose a key portion of the dynactin complex, termed the projecting arm. To investigate the roles of the dynactin complex in mitosis, we used RNA interference to down-regulate p24 and $p150^{Glued}$ in human cells. In response to p24 down-regulation, we observed cells with delayed metaphase in which chromosomes frequently align abnormally to resemble a "figure eight," resulting in cell death. We attribute the figure eight chromosome alignment to impaired metaphasic centrosomes that lack spindle tension. Like p24, RNA interference of $p150^{Glued}$ also induces prometaphase and metaphase delays; however, most of these cells eventually enter anaphase and complete mitosis. Our findings suggest that although both p24 and $p150^{Glued}$ components of the dynactin complex contribute to mitotic progression, p24 also appears to play a role in metaphase centrosome integrity, helping to ensure the transition to anaphase.

The dynein-dynactin complex, a minus end-directed microtubule-based motor, carries out diverse transport activities indispensable for various cell functions and behaviors (Ref. 1 and references therein). For instance, the dynein-dynactin complex transports giant centrosomal scaffold proteins such as CG-NAP/AKAP450 and NuMA and induces smooth progression through mitosis. This motor complex also contributes to the transition from metaphase to anaphase: To ensure that each daughter cell receives only one chromosome set, the spindle assembly checkpoint blocks entry into anaphase until kinetochores on sister chromatids are attached to opposite spindle poles. Once this condition is achieved, the dynein-dynactin motor induces passage through the spindle checkpoint by removing critical checkpoint proteins (such as BubR1 or Mad2) from kinetochores.

* This work was supported by grants-in-aid for scientific research from the Ministry of Education, Culture, Sports, Science and Technology of Japan.
[S] The on-line version of this article (available at http://www.jbc.org) contains supplemental Movies 1–3.
[1] To whom correspondence should be addressed: 1-2-3 Kasumi, Minami-ku, Hiroshima 734-8553, Japan. Fax: 81-82-256-7103; E-mail: tinaba@hiroshima-u.ac.jp.

Dynactin is composed of 10 subunit proteins that are required for dynein activation (2) and references therein). Three proteins among them, $p150^{Glued}$ (dynactin 1), dynamitin (p50 and dynactin 2), and p24 (dynactin 3) (3, 4), constitute a flexible and extendable structure (the projecting arm) that associates directly with microtubules and the dynein complex.

Each dynactin molecule contains two copies of $p150^{Glued}$ and p24 and four copies of dynamitin. All three proteins are evolutionarily conserved from yeast to mammalian cells (5, 6), suggesting that these components are essential for the formation of a functional projecting arm. Within this substructure, $p150^{Glued}$ is sufficient for binding to dynein and for traversing the microtubule lattice, whereas dynamitin also plays a critical role in association with the dynein complex and in promotion of dynein-based movement. It is noteworthy that overexpression of dynamitin disrupts dynactin structure (7). Although the mechanism underlying this disruption is yet to be elucidated, dynamitin overexpression has been the major tool in molecular biology for down-regulation of dynactin function (2). Indeed, dynamitin overexpression was used to verify involvement of the dynactin complex in the spindle checkpoint silencing that induces metaphase arrest/delay (8).

In contrast to $p150^{Glued}$ or dynamitin, little is known about the role of the p24 subunit in mitosis. Although Ldb18 (a *Saccharomyces cerevisiae* homolog of p24) is essential for attachment of $p150^{Glued}$ to dynamitin and to the remainder of the dynactin complex (6), low amino acid identity between Ldb18 and human p24 (16.9%) does not favor speculation on the roles of mammalian p24.

RNAi is currently the most useful method for down-regulating the expression of a specific gene. Although several authors report successful suppression of $p150^{Glued}$ using siRNA or shRNA (8–10), their papers did not describe any mitotic abnormalities in cells expressing reduced levels of $p150^{Glued}$. Moreover, there have been no reports of p24 down-regulation using the RNAi method. In this report, we use RNAi to down-regulate p24 and $p150^{Glued}$ proteins in human cells. Our results demonstrate that cells expressing reduced levels of either p24 or $p150^{Glued}$ both show severe metaphase delay but that other mitotic disturbances differ between the two suppressed genes.

EXPERIMENTAL PROCEDURES

Cell Culture and Transfection of siRNA—HeLa, U2OS, and HEK 293 cell lines and their derivative cells were cultured in Dulbecco's modified Eagle's medium supplemented with 10% FBS. siRNA oligonucleotides for $p150^{Glued}$ (siRNA-p150, 5′-